# Building system-of-systems methodologies for interdependent network creation

## Deliverable D2.2

**Release Status:** FINAL
**Dissemination Level:** Public
**Authors:** Alberto Fernandez Perez, Raghav Pant, Milos Pantos, Yue Li, Tom Russell, Fred Thomas, Jim W. Hall
**Date:** 16-12-2024
**FIle name and Version:** D2.2 MIRACA.pdf
**Project ID Number:** 101093854
**Call:** HORIZON-MISS-2021-CLIMA-02-03
**DG/Agency:** CINEA

This project has received funding from the European Union's Horizon Europe research and innovation programme under grant agreement No. 101093854

# Executive Summary

This document helps to understand cross-sectorial interdependencies within critical infrastructure (CI) networks at pan-European scale. It fulfills the requirements of Task 2.2 within Work Package 2 (WP2) of the Multi-Hazard Infrastructure Risk Assessment for Climate Adaptation (MIRACA) project. The main outcome of this document is a proposed comprehensive framework and methodology for mapping and analyzing cross-sectorial interdependencies of lifeline infrastructure networks across Europe, emphasizing cascading risks and resilience.

The document: (1) identifies and classifies interdependencies between critical infrastructure networks of transport, energy and telecoms, (2) provides a functionality-based mapping of the different network components at the different sectors, categorizing assets as sources, intermediates, or sinks, and detailing the services exchanged between networks, (3) develops a hierarchical system-of-systems framework that outlines the process for mapping the connectivity and flow of resources, commodities, passengers and information within and across CI networks, and (4) provides a process of modelling cascading failures across networks and assembling vulnerability and resilience metrices that track across interdependent failure mechanisms.

The interdependency methodology involves understanding the role of network components and how their failure or performance impacts other networks. Key features of the methodology include:

- Functionality-Based Asset Mapping: In which assets are categorized based on their role in maintaining network functionality—whether as producers, transmitters, or consumers of resources or services.
- Hierarchical System-of-Systems Representation: Which involves models of cascading flow disruptions through interdependent layers of networks, reflecting both direct and indirect impacts.
- Scalable Analysis Framework: Provides tools for analyzing risks and dependencies at both regional and European scales.
- Cascading Failure Modeling: Enables understanding of how disruptions propagate through interconnected systems.
- Impact and Resilience Metrics: Develops metrics to assess disruptions at the asset level, accounting for functionality loss and cascading impacts across networks and sectors. These metrics allow for a better understanding of how localized disruptions affect broader systems and enable the creation of effective resilience strategies.

The creation of an interdependent network flow and failure analysis methodology is followed by the compilation of relevant pan-European datasets to transport (roads, railways, maritime and inland waterways and ports, airlines and airports), energy

This project has received funding from the European Union's Horizon Europe research and innovation programme under grant agreement No. 101093854

(electricity and gas) and telecommunications that will be utilized for implementation in the next phases of the MIRACA project. The document demonstrates that the proposed methodology is feasible at the pan-European scale, by showing how the proposed CI datasets will the converted in interconnected networks.

Network flow models, that are being developed in MIRACA, are also discussed in this document with the relevant compilation of proposed datasets and approaches to create origin-destination (OD) flow matrices for transport networks and supply-demand balance models for energy and telecoms networks. These models provide a process-based understanding of flow allocation and failure propagation to show how CI service delivery would affect customers (commodities, people, businesses).

The document concludes by discussing the value of the proposed methodology, while recognizing the challenges and limitations in created harmonized pan-European interdependency data and models. Next steps of the development and implementation of the methodology and its integration with the other Work Packages of MIRACA are also discussed.

This project has received funding from the European Union's Horizon Europe research and innovation programme under grant agreement No. 101093854

# Table of contents



This project has received funding from the European Union's Horizon Europe research and innovation programme under grant agreement No. 101093854

# 1. Introduction

The resilience of critical infrastructures (CI) is essential for maintaining the services that underpin everyday socio-economic activities. Critical infrastructure systems—such as electricity, digital communication, transportation (roads, railways, maritime and inland waterways, airports) and gas—form interdependent networks, and assessing their vulnerability and resilience requires understanding how failures in one system can trigger cascading effects across others. A system-of-systems approach is needed to unravel the interdependency patterns, drawing on data about the physical structure, operations, and failure patterns of real-world networks. Such analysis enables better decision-making by providing insights and tools to geospatially identify vulnerable assets and locations that have the greatest impact on overall system performance. Understanding interdependency, potential cascading modes, and their consequences is therefore crucial for acting to enhance infrastructure resilience.

In the context of the Multi-Hazard Infrastructure Risk Assessment for Climate Adaptation (MIRACA) project, a methodology is needed to evaluate the interdependencies between the main modes of transportation, energy and information resources required for their proper functioning. The approach should progress from an understanding of the asset scale functions towards network scale functions, beginning with an assessment of relationships within individual CI in the same network and then exploring interdependencies between different networks, as shown in Figure 1.

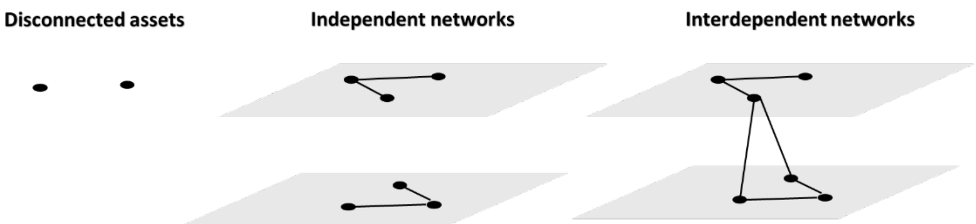


**Figure 1:** Schematic representation of the build-up towards an interdependent model

This methodology does not only identify interdependencies but also analyzes it how they influence the impact and disruption propagation between different sectors, while characterizing the network losses resulting from cascading effects.

To develop a methodology that fulfills the objectives of WP2, Task 2.2 outlines (through this report) a comprehensive technical approach for MIRACA towards identifying key connections and dependency patterns between the main transportation, energy, and telecommunication sectors. This will enable the

This project has received funding from the European Union's Horizon Europe research and innovation programme under grant agreement No. 101093854

characterization of spillover effects towards people and economic activity driven by extreme hazards impacts. The methodology approach developed in this study involves:

1. Defining an interdependency framework as a baseline.
2. Establishing data that would be needed to evaluate the interdependencies between different CI networks.
3. Creating models to assess impact propagation within and between CI networks.
4. Defining impact metrics across sectors to inform systemic failure impacts.

The report is structured as follows: Section 2 presents the framework for interdependency analysis with relevant output metrics, Section 3 outlines the data needs for evaluating cross-sectoral interdependencies, Section 4 details the flow allocation models, and Section 5 concludes with key insights and future work.

This project has received funding from the European Union's Horizon Europe research and innovation programme under grant agreement No. 101093854

# 2. Interdependency framework

## 2.1. Suitable approaches for interdependency modelling

Developing comprehensive models that fully capture the complexity of interdependent transport, energy and telecoms systems is challenging. The Task 2.1 report of MIRACA project reviewed the state-of-the-art in the modelling principles of CI system-of-systems (Pant et al., 2024). Relevant interdependency types were identified, as shown in Table 1, which are to be translated into a model for capturing and quantifying failure propagation across multiple CIs.

**Table 1:** Description of different types of interdependencies identified as relevant for CI systems (Pant et al., 2023).

| Interdependency type | Definition | Practical applications in MIRACA |
|---|---|---|
| Physical | Different CI assets are physically connected and share inputs and outputs with each other. | Electricity network CI asset failures shutting down directly connected CI assets transport, telecommunications, schools and hospitals. |
| Geographic/Geo-located/ Spatial | CI assets are exposed to the same local environment or spatial footprint. | A large flood hazard destroying road bridges, which might also have electricity and telecoms cables going under it. |
| Cyber/Informational | There is an exchange of information between CI assets, underpinned by an information infrastructure. | Telecom data center failures shutting down operations of electricity networks, emergency health services, and road and railway signaling. |
| Functional (combination of physical and cyber) | The operation of CI assets of two infrastructures are contingent on the supply of resources and services from each other. | Electricity and telecommunications CI asset failure shutting down both networks and affecting operations for transport, education and health CI assets. |

Various modeling approaches were reviewed, such as network science, macroeconomic Input-Output, and agent-based models. Task 2.1 report concluded that the most suitable approach for CI systems modelling in MIRACA at the pan-European scale would be the one that combines network science models with population and resource flow allocation models. This conclusion is supported by the availability of relevant pan-European data (discussed later in the report) and demonstrable models for transport, energy and telecoms networks in Great Britain (Pant et al., 2020), electricity and gas networks for Europe (Poljanšek et al., 2012), transport networks globally (Koks et al., 2023) and in Vietnam (Oh, J. E. et al., 2019)

This project has received funding from the European Union's Horizon Europe research and innovation programme under grant agreement No. 101093854

and Argentina (Kesete et al., 2021). The development of a network-based methodology for interdependent CI analysis is explained next.

## 2.2. System-of-systems network modelling

Critical infrastructure systems-of-systems are defined as interconnected networks of physical facilities and human systems that work together to deliver infrastructure services (Hall et al., 2016). This definition is particularly relevant to our study, since it focuses on understanding the dependency of society and economy on the CI networks. The next subsections explain how this definition is translated into a formulation that help quantify the system-of-systems attributes for service delivery and failure propagation.

### Network formulation

In graph theory, , a *network* is defined as a collection of nodes connected by a set of edges (Cohen & Barabási, 2002; Lewis, Ted G., 2011). *Nodes* represent key locations within infrastructure systems, such as electricity substations or rail stations. *Edges* represent the physical connections between nodes, such as power lines, road sections, or railway tracks. They may also represent notional connections, indicated by straight lines between nodes to reflect non-physical interactions such as information exchange. The structure or arrangement of these nodes and links is referred to as the *network topology*. For a network comprising $v$ nodes and $w$ edges, the graph can be expressed as a set $I = \{N, E\}$, where: $N = \{n_1, \dots, n_v\}$ is the set of nodes, $E = \{e_{11}, \dots, e_{ww}\} = \{e_{ij} \rightarrow (n_i, n_j) | \forall i, j \in [1, v]\}$, is the set of edges defining which nodes $(n_i, n_j)$ are connected to each other. This structure highlights both the arrangement of nodes and the physical or logical connectivity of edges, forming the basis for analyzing interdependencies within and across infrastructure networks. The nodes and edges are also co-located in space, which captures the aspect of geographic interdependencies.

To understand how networks deliver services, in addition to the topology, the functional attributes of nodes are required to determine the direction of resource flows (Thacker et al., 2017a). The network model includes three types of node functions: (1) source/origin nodes, where network services are generated; (2) sink/destination nodes, where services are delivered or end; and (3) intermediary nodes, which transmit services from sources to sinks. Such nodes could all be within the same infrastructure network or across multiple infrastructure networks. Connecting source nodes to intermediary nodes or intermediary nodes to sink nodes, results in creating directed edges.

This project has received funding from the European Union's Horizon Europe research and innovation programme under grant agreement No. 101093854

The flow of resources is traced along directed paths connecting a chosen source to a sink, incorporating all assets traversed along the way. Mapping all possible directed flow paths provides a comprehensive functional (inter)dependency that captures how the network topology and function supports service flows. A depiction of the topology definition and functional dependency edges across networks is shown in Figure 2.

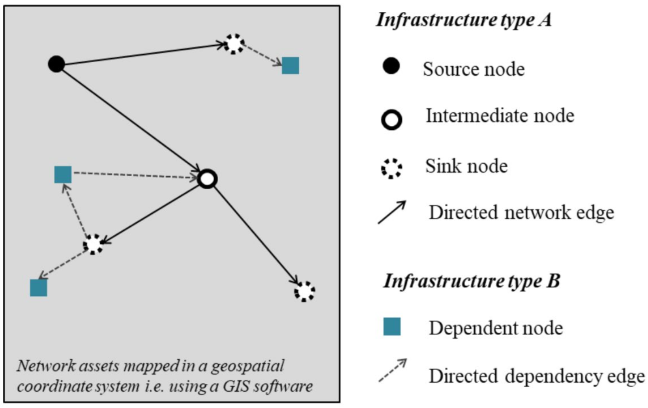


**Figure 2:** Representation of network typology and functional dependencies (from Pant et al. (2020))

## Connecting the networks

CI networks span multiple scales and geographies, resulting in many sources, intermediate and sink nodes that are functionally interdependent. To simplify the understanding of CI interconnectedness, networks have been conceptualized to exist in a layered hierarchy (Thacker et al., 2017a; Verschuur, Pant, et al., 2022). Larger nodes with broader, supranational-level influence are positioned at the top, while smaller, locally influential nodes are at the bottom, as shown in Figure 3. Multilayered network models have been shown to explain failure cascade mechanisms across spatially embedded interdependent networks better than single layered network models (Buldyrev et al., 2010; Kivela et al., 2014).

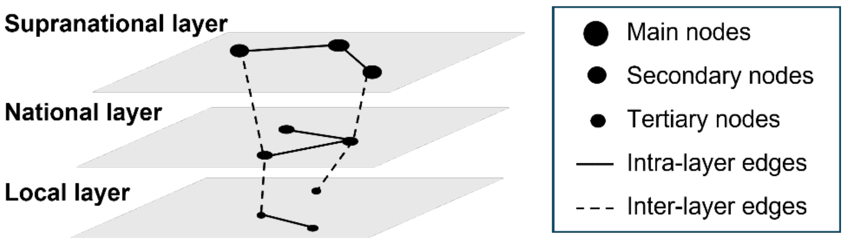


**Figure 3:** Representation of hierarchical network typology and dependencies

The main goal of the present study is to model the bidirectional relationships between the cross-sectorial CI networks, modelling how the disruption of resource

This project has received funding from the European Union's Horizon Europe research and innovation programme under grant agreement No. 101093854

(electricity, gas and telecoms) networks affect the systems operability and how the disruption of the transportation (road, rail, waterways and air) networks affect the systems accessibility. To do so, not only the hierarchical network connections should be characterized for each sector (mode), but also between sectors (modes) at different hierarchical layers, as shown in Figure 4 (adapted from Thacker et al. (2017)).

Based on those connections, the cross-sectorial interdependencies are coherently mapped, evaluating the passenger, commodities, energy and information flows within and between networks, which is the preliminary step to evaluate the cascading impacts due to localized failure of single or multiple nodes.

Extending the mathematical nomenclature of the graph, to represent interdependent infrastructure sectors $S = \{1,2,\dots,g\}$ results in the system-of-systems graph being formulated as the set $I = \{N, E\}$, where: $N = \{n_1^1, \dots, n_v^g\}$ is the set of nodes, $E = \{e_{ij}^{sl} \rightarrow (n_i^s, n_j^l) | \forall\, i,j \in [1,v], s,l \in [1,g]\}$, defining which nodes within or across sectors $(n_i^s, n_j^l)$ are connected by each edge $(e_{ij}^{sl})$.

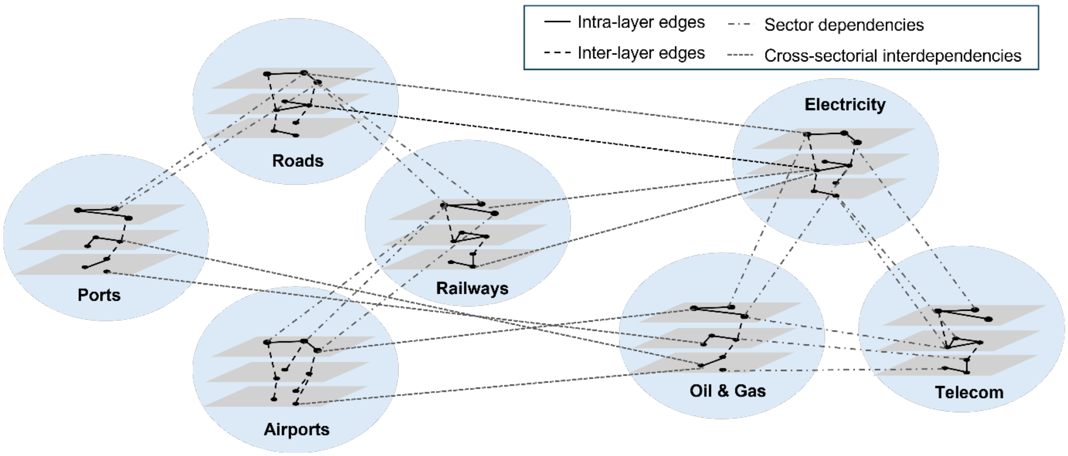


**Figure 4:** Representation of multi-modal and cross-sectorial network typologies and dependencies (adapted from Thacker et al., 2017)

## 2.3. Nature of functional interdependencies mapping

Before developing interconnected CI network models, it is important to understand the nature of functional interdependencies that can be feasibly mapped and represented with available data. Network interdependencies data are highly challenging to collect due to two main reasons: (1) there are no established practices or regulations requiring network operators to share data on their links to other networks, unlike the practice of making some of their own network data open access; and (2) many operators lack information beyond their own networks. As a result, most interdependencies are represented by creating notional edges between network assets, given the limited information on actual physical connections (e.g., cables, pipes) between sectors. These edges account for both the physical (inter)dependencies among networks and the cyber dependencies related to the digital communication (telecom) network. As a preliminary approach, a feasible mapping of interdependencies is proposed (see Figure 5) to highlight the essential interconnections that need further investigation to understand cross-sector resilience (Zorn et al. 2020). The figure depicts two types of functional linkages that are created through notional edges:

- **Accessibility linkages:** This refers to the ability of assets within a transport network to connect or interact with assets in another network. For example, accessibility might involve cargo reaching a port by road for shipment to power plant or maintenance crews accessing a substation via road to perform repairs. These interactions rely on functional routes; thus, a failure in the road network (e.g., a road edge disruption) could obstruct such essential inter-network connections.
- **Operability linkages:** This refers to the operational functionality of assets within all networks being dependent on the delivery of service from assets of the resource networks. For instance, the operability of a railway system may rely heavily on continuous power supply from the electrical grid and connectivity through telecommunication networks. Disruptions in these supporting networks can directly impact the railway's ability to function effectively.

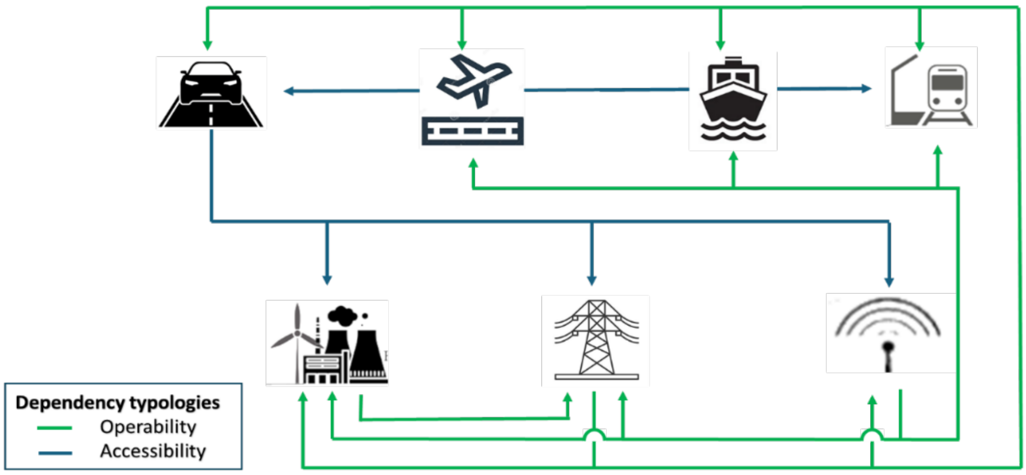


**Figure 5:** Functional linkages diagram for the cross-sectorial dependency analysis (from Zorn et al. 2020).

Figure 5 represents the types of operational and accessibility linkages that could be established, when notional edges are created between CI assets by assuming connections based on node spatial proximity in the absence of physical asset information. This assumption aligns with the general understanding that infrastructure services are most efficiently delivered by connecting nearest assets with each other (Pant et al., 2020; Thacker et al., 2018). However, connectivity can also be extended to the next *k*-nearest assets in cases where the nearest asset

This project has received funding from the European Union's Horizon Europe research and innovation programme under grant agreement No. 101093854

might not have the required capacity to provide service and in cases where the networks are designed to have redundancy in supply (Pant et al., 2020).

Because the notional edges would be inferred based on proximity mapping, they are approximate. It should be acknowledged that if a source, intermediate or sink node was inaccurately identified due to missing data, dependent assets might connect to the network at incorrect locations—a likely outcome in this approach.

**Table 2:** Types of dependencies considered in the analysis (adapted from Pant et al. (2020))

| Dependency edges (from-to) | Operational and accessibility linkages |
|---|---|
| Electricity-rail | - Data collected on electricity point assets along railways network<br>- Electricity traction substations (nodes) connected to rail nodes with known information on route<br>- Other electricity points connected to rail stations/rail tracks based on proximity<br>- Electricity traction substations connected to the rest of the electricity network |
| Electricity-road | Road lighting assumed dependent on their nearest low voltage substation |
| Electricity-airports/ports | Electricity traction substations connected to airports and ports tracks based on proximity |
| Electricity-IWW | - Data collected on electricity point assets along channels network<br>- Electricity traction substations (nodes) connected to inland ports and locks based on proximity<br>- Electricity traction substations connected to the rest of the electricity network |
| Electricity-telecoms | Telecom assets are assumed dependent on their nearest low voltage substation |
| Electricity-gas | - Electricity substations (nodes) connected to compressors, LNG stations and storage stations based on proximity<br>- Electricity High Voltage substations rely on Gas Power Stations (Consumers of Gas Network) |
| Telecoms-rail | - Data on telecom masts along existing rail network<br>- Telecoms masts (nodes) connected to nearest rail nodes based on proximity<br>- Internet Exchange Points (IEPs) are critical nodes for the telecom network. Rail network connected to the closest one |
| Telecoms-airports/port | - Telecoms masts (nodes) connected to nearest airport/port based on proximity<br>- Internet Exchange Points (IEPs) are critical nodes for the telecom network. Ports and airports connected to the closest one<br>- For IWW, locks connected to closest mast |
| Telecoms-electricity | Electricity nodes dependent to their nearest IEP and masts |
| Telecoms-gas | Mast, comms towers and IEP connected to compressors, LNG stations and storage stations based on proximity |

This project has received funding from the European Union's Horizon Europe research and innovation programme under grant agreement No. 101093854

| | |
|---|---|
| Road-electricity | Access to substations and main nodes based on proximity of the closest road edge, tracing back potential paths to the closest motorway (main road) |
| Road-telecom | Access to masts and IEP based on proximity of the closest road edge, tracing back potential paths to the closest motorway |
| Road-gas | Access to compressors, LNG stations, storage stations and pipes based on proximity of the closest road edge, tracing back potential paths to the closest motorway (main road) |

## 2.4. Interdependent failure estimation models

### Failure cascading identification

After creating the multi-layered network models and identifying the types of functional interdependencies between networks, the failure propagation (cascading effects) analysis involves the removal of nodes and/or links that are affected by climate related events (i.e., floods, droughts, etc.), and the evaluation of the change to network flows due to their removal, jointly with the evaluation of the flow variation across networks. In this analysis, it is assumed that a failure results in a loss of service at a node. There could be partial failures, where nodes continue to operate at less than full capacity and provide diminished service, and in the most extreme-case nodes suffer complete failures resulting in worst-case scenarios involving large-scale disruptions. The cascading effects of failures can unfold in two ways: (1) they can affect nodes and edges in the immediate vicinity of the initiating asset, and (2) they can impact more distant assets that cease to receive service due to flow paths being interrupted by the failure of the initiating asset

After the initiation of failures on nodes and edges, network flow models allow to adjust to disrupted state flows with the new topologies. First, for the disrupted network, then for the dependent networks. Network-specific flow models are discussed in detail later in this report, while the focus here is to develop the process of cross-sectoral failure propagation.

To capture the cascading effects of interdependent network failures, we differentiate between the network where the initiating event occurs and the subsequent propagation of failures to other networks. Figure 6 illustrates a schematic representation of service demand disruptions in the network where the initiating event takes place (marked with the big X), while cascading service demand disruptions occur in dependent networks due to the loss of service from the initiating failure network.

This project has received funding from the European Union's Horizon Europe research and innovation programme under grant agreement No. 101093854

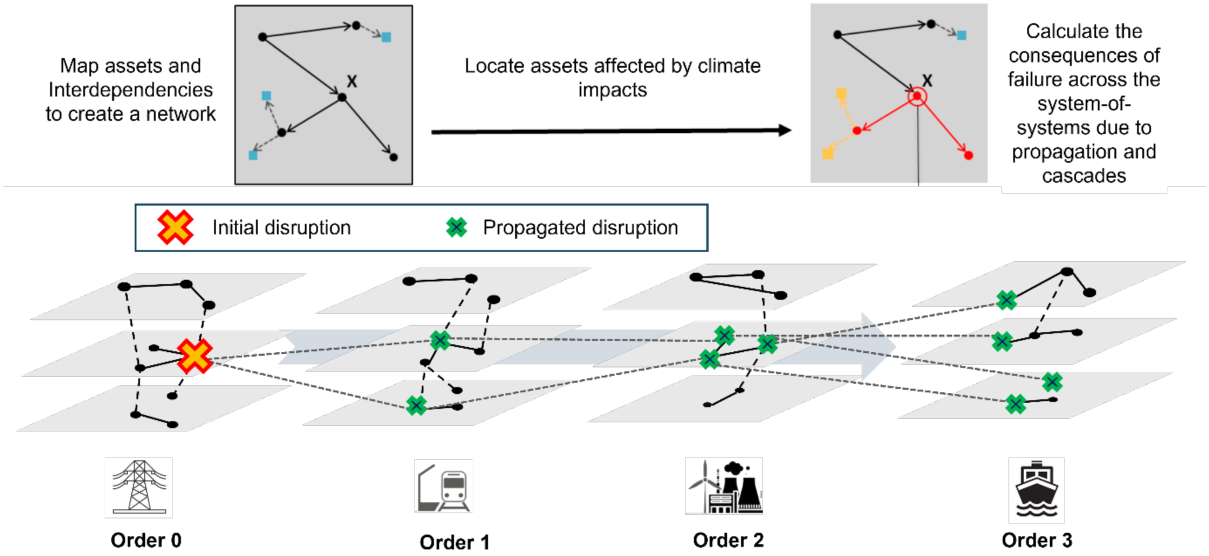


**Figure 6:** Representation of initial and cascading service disruptions across interdependent networks

This study will focus on tracking the number of failure sequences that lead to cascading service demand disruptions. Therefore, we use the term "Order 0" to indicate an initiating service disruption effect, and "Order n" (>0) to monitor further sequences of cascading service demand disruptions. In the hypothetical example depicted in Figure 6, there is an initiating (Order 0) failure of pylons and overhead lines in the electricity network, which propagates to the railway network (Order 1) then feeds into the gas network (Order 2) by affecting operations of power plants (due to delays or lack of access) and further affects some of the operations of the shipping network (Order 3) that rely of the supply of electricity from the power plants.

Studies at national and international scales have demonstrated that mapping disruptions by orders is useful from capturing the behavior of CI interdependencies (Mühlhofer et al., 2024; Pant et al., 2020; Thompson et al., 2024). Differentiating these orders of disruption clarifies how failure can propagate through interdependent sectors across space and time. This could provide critical insights in pinpointing vulnerable nodes and edges that uphold multiple pan-European CI networks.

### Impact assessment and vulnerability metrics

The impact of failures or network vulnerability refers to the extent of service provision affected by the failure of network nodes and edges due to external shock events (Pant et al., 2016, 2020). In this study, the affected service provision will be quantified by the total value of lost services, which could either be in terms of the numbers of people affected by reduced and lost service or in terms of the economic cost of the flow reduction in the whole network. Metrics per sector and aggregated

This project has received funding from the European Union's Horizon Europe research and innovation programme under grant agreement No. 101093854

metrics for cross-sectorial loses can be computed at different spatial and temporal levels.

To evaluate vulnerability of the multi-layered interdependent infrastructure networks subjected to an external hazard shock $(H)$, the operational state of an individual node (or edge) can be quantified using a state function, $r_i^s$ (or $r_{ij}^{sl}$), which can take values within the range [0,1] to signify the level of operability of the node (or edge). Here $r_i^s = 1$ (or $r_{ij}^{sl} = 1$) represents full functionality and $r_i^s = 0$ (or $r_{ij}^{sl} = 0$) indicates complete failure.

The overall state of a network disrupted by the hazard is represented by the set $R\,(H) = \{r_i^s(H)\} \cup \{r_{ij}^{sl}(H)\} \forall i, j \in [1, v], s, l \in [1, g]$. If the network's state is represented such that at least one asset has a state value < 1, the corresponding negative consequences serve as a measure of the network's vulnerability. Assessing this vulnerability requires accounting for physical and functional propagation effects. These effects refer to the reduction in network service levels due to disrupted physical connections and impaired functional relationships among interconnected assets.

The service flow of disrupted network is expressed as $f^s(R^s)$, where $f^s()$ is a function that represents a flow model of sector $s$ that aggregates individual asset flows for a given state of operation into a measure of total network service flow.

Network vulnerability of an individual CI or interdependent CIs is represented as a two-dimensional global metric that evaluates two critical aspects:

- **Degree of Operational Failure:** This measures the proportion of network assets that are non-operational due to the external hazard shock. Represented mathematically, if the network's full operational state adds up to $a = |R|$ and operational state due to the hazard is denoted by $R\,(H) = \{r_1, \dots, r_a\}$, the degree of operational failure $\theta(H)$ is calculated as:

$$\theta(H) = \frac{\sum_{z=1}^{a}(1 - r_z(H))}{a} \qquad [1]$$

  Here, $\theta(H)$ is a normalized global metric, where $\theta(H) = 1$ indicates the network is entirely operational, and $\theta(H) = 0$ signifies total network failure.

- **Relative Magnitude of Disruption Consequences:** This aspect assesses the functional impact of disruptions. It is expressed as the ratio of service loss (customers disrupted or economic activity disrupted) after a disruption to the service level before the disruption. If the pre-disruption service level is $f(P)$, and the service level after a disruption in state $R\,(H)$ is $f\,(R\,)$ then the relative magnitude of disruption $\Phi(H)$ is given by:

$$\Phi(H) = 1 - \frac{f\,(R\,)}{f(P)} \qquad [2]$$

  This normalized metric ranges from $\Phi(H) = 0$, indicating no loss of service, to $\Phi(H) = 1$, indicating total loss of service.

This project has received funding from the European Union's Horizon Europe research and innovation programme under grant agreement No. 101093854

These metrics are combined to form the overall network vulnerability metric for a given state vector set $R$:

$$\Psi\,(H) = [\theta(H), \Phi(H)] = \left[\frac{\sum_{z=1}^{a}(1-r_z(H))}{a}, 1 - \frac{f\,(R\,)}{f(P)}\right] \qquad [3]$$

Since both components are normalized, this approach enables comparisons across different types of disruptions and performance metrics.

The approach can also help track the order of component failures and the network losses to track cascading impacts. In a cascading failure scenario, the state function can include information of the set of orders of the failures $O = \{1, \dots, o\}$.

$$\begin{aligned} & R(H, O) \rightarrow \\ & \rightarrow R(H, 0) = \left\{\{r_i^s(0)\} \cup \{r_{ij}^{sl}(0)\}\right\} \rightarrow \\ & \rightarrow R(H, 1) = \left\{\{r_i^s(1)\} \cup \{r_{ij}^{sl}(1)\}\right\} \rightarrow \cdots \rightarrow \\ & \rightarrow R(H, o) = \left\{\{r_i^s(o)\} \cup \{r_{ij}^{sl}(o)\}\right\} \end{aligned} \qquad [4]$$

An ordered assessment of vulnerability can be constructed:

$$\Psi\,(R(H, O)) = \big(\Psi\,(R(H, 1)), \dots, \Psi\,(R(H, o))\big) \qquad [5]$$

This provides a detailed representation of the potential impacts and consequences of failures, supporting a thorough analysis of network resilience.

### Dynamic resilience

The vulnerability metrics can be estimated temporally to also account for the evolution of failure and recovery across networks. This would provide an understanding of the dynamic resilience of networked systems (Rose, 2004; Xie et al., 2018). Some of this resilience would be due to the stabilization of flows across network following rerouting or redistribution of resources.

For operability linkages, some dynamic resilience behavior would be capture by accounting for redundancy, or backup supply, where for a certain duration dependent assets could continue operating using an alternative supply of the same service. For example, a 24-hour backup (e.g., via electric generators) could assumed for critical nodes, such as Internet Exchange Points, LNG and storage stations, tunnels, ports, airports, and intermodal terminals (Pant et al., (2020)). For telecom backup, redundancy is incorporated through network design, enabling triangulated connections with other nodes. This redundancy applies to critical nodes like intermodal terminals, substations, airports, and ports.

In terms of accessibility linkages, redundancy is achieved by providing suboptimal, non-shortest-path alternatives for reaching essential assets in case primary routes are disrupted.

This project has received funding from the European Union's Horizon Europe research and innovation programme under grant agreement No. 101093854

To account for backup supply and temporal disruption dynamics, the evolving service disruption metrics or dynamic resilience could be measures across roughly four timeframes in the impact analysis:

- Pre-disruption phase: Represents baseline service levels under normal conditions, with all sectors fully operational.
- Immediate after disruption phase: Captures service levels directly following the disruption, reflecting reduced flows due to eliminated nodes and edges but considering functional backup supplies. Limited flow reallocation occurs at this stage.
- Stabilized after-disruption phase: Reflects service levels after backup supplies are depleted and all flows are reallocated to remaining operational nodes, edges, and modes.
- Recovery phase: Reflects service levels being restored as more failed assets are fixed and brought into the set of operational nodes, edges, and modes.

Figure 7 illustrates service variation across these timeframes. In the first few hours or days, transport service levels drop significantly due to disrupted infrastructure but begin to recover as flows are redistributed. Resource flows, initially stable due to backup supplies, face sharp declines once these reserves are exhausted, leading to further service degradation. This timeline underscores the critical role of backups and the lagged recovery facilitated by flow reallocation.

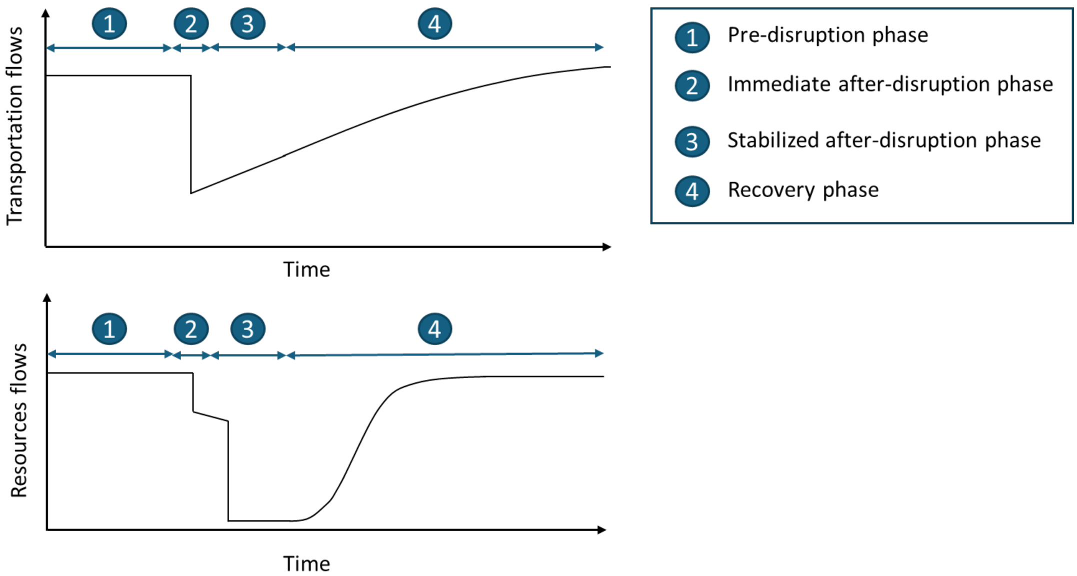


**Figure 7:** Multi-stage flow variation analysis for interdependent transportation and resources networks

This project has received funding from the European Union's Horizon Europe research and innovation programme under grant agreement No. 101093854

## 2.5. Interdependency framework implementation

Following the creation of the model formulations the proposed implementation of the interdependency framework or MIRACA is presented. Figure 8 shows the flowchart of the framework, where a separation has been made between transport networks and resources networks, to make the distinction between the types of flow models that will be needed for these different types of networks. The process starts with the topology allocation of individual networks, progresses to interconnected networks, and finally establishes the entire interdependency structure across all sectors. A modular methodology is coherently defined based on the following common input components:

1. **Location data collection for individual networks (exposure data)**: Spatial nodes and edges datasets with attributes such as point, line and polygon locations and dimensions are identified for both transportation (ports, airports, roads, and railways) and resource networks (electricity, telecom and gas). Spatial accuracy is key for interdependency analysis as it quite a reliable indicator for inferring interconnectedness, because some assets would connect based on spatial proximity.
2. **Function properties of assets**: Data such asset functional characteristics (transport hubs, source, intermediate and sink nodes), flow attributes (capacities, operational constraints) are collected across transportation and resources networks. These datasets help infer physical, geographic and logical (leading to functional) relationships between nodes and edges within and across different networks. This would help quantify how networks would exchange resources or share spaces to facilitate redistribution of commodity/passengers.
3. **Transport origin-destination and resource flow matrices data for analysis**: Data for and initial model setup are collected for estimating flows within and across networks. Transport flows (passenger and commodity movements) are estimated from origin-destination (OD) matrices, which provide some understanding of movements between specific node locations or between high-level administrative boundaries. Similarly, resource flow matrices data (electricity, telecom and gas usage) at specific node locations or administrative areas are collected to model resource flows. These flow models will help understand how impacts propagate within and across networks.

The proposed implementation of the interdependency framework shown in Figure 8 will be done by first implementing individual network modules shown at the left and right ends of the flowchart (in green and grey), then moving towards the implementation of multi-modal transport module (shown in blue) and cross-sectoral resources network module (shown in pink), and finally connecting all models into a

This project has received funding from the European Union's Horizon Europe research and innovation programme under grant agreement No. 101093854

full cross-sectorial interdependency model leading to a cascading failure model, driven by external hazard shocks.

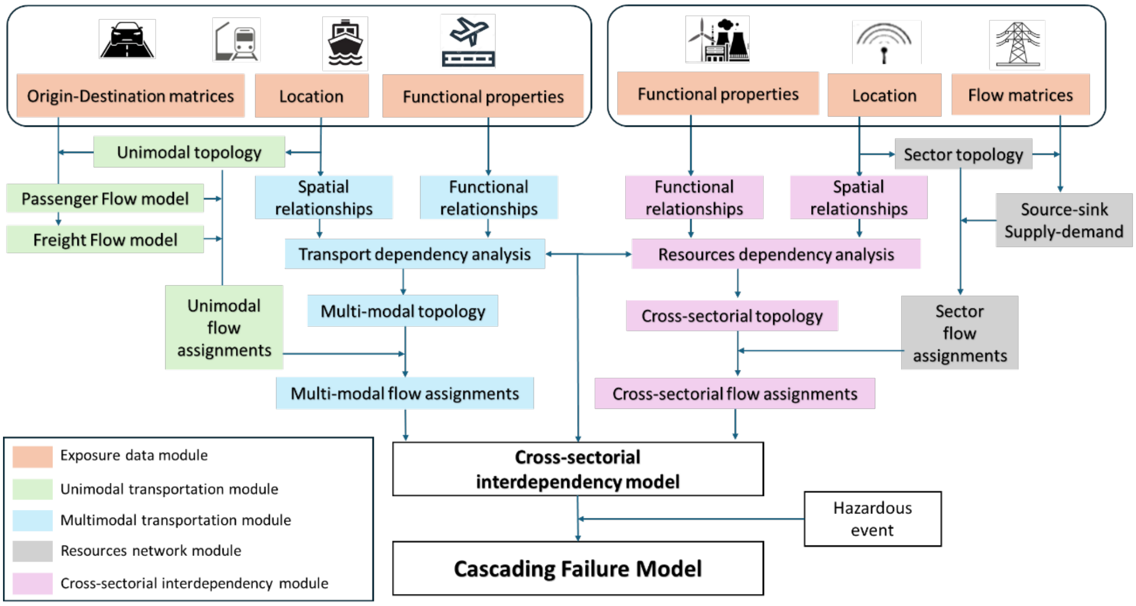


**Figure 8:** Workflow for the multi-modal interdependency analysis

This project has received funding from the European Union's Horizon Europe research and innovation programme under grant agreement No. 101093854

# 3. Data for interdependent network assessment

Following the formulation of the system-of-system model for interdependent CI network, the data that would be required to implement the model at a pan-European scale is assembled and reviewed. As defined by the interdependency framework, assessing cross-sectoral impact propagation requires characterizing the dependency structure between different CI network, which in our case include transportation (road, rail, ports and airports) and resource (electricity, gas and telecoms) modes.

## 3.1. Data gathering

The first step in the methodology involves obtaining the exposure data for infrastructure networks, including transportation (roads, railways, ports, and airports) and resources (electricity, telecom and gas). This process begins by exploring the key databases identified in another Work Package (WP1) of MIRACA to select the most relevant ones for the interdependency analysis. To date, there is no homogenized database for CI networks at pan-European level in terms of location and topology definition. For that reason, in this study (coherently with the databases obtained at WP1), OpenstreetMap, UNECE Infrastructure Census, SciGrid (IGGIELGN), OGIM, Emodnet and EuroRegionalMap databases are explored. For most networks, a hierarchical layer structure is found, which helps to define the topology of the network. In Table 3 (for transportation networks) and Table 4 (for resources' networks), the main located databases are depicted, including the hierarchical layers and the features described in each one.

Figure 9 and Figure 10, showing samples of the data for Belgium, demonstrate that the spatial resolution of the original datasets is detailed enough to analyze functional dependency patterns between networks. Moreover, the cross-border links are precisely mapped, allowing for a thorough pan-European analysis to evaluate cross-sectoral vulnerabilities across the continent.

The multi-layered network representations of the networks are shown in Figure 11. For the interdependency analysis, spatial integration of all networks is essential, functional dependencies are typically location-specific. The process involves integrating transportation modes and examining their interconnectedness and also resource networks are incorporated to create a comprehensive cross-sectoral, interdependent network.

This project has received funding from the European Union's Horizon Europe research and innovation programme under grant agreement No. 101093854

**Table 3:** Databases selected for the transportation network analysis, as the basis of the interdependency analysis

| Transportation mode | Source | Hierarchical Layers | Features |
|---|---|---|---|
| Roadways | OpenstreetMap | Motorways<br>Primary roads<br>Secondary roads<br>Tertiary roads | Lanes<br>Max Speed<br>Bridge/Tunnel<br>Width<br>Service |
| Railways | OpenstreetMap | Main railways<br>Secondary railways | Max Speed<br>Voltage<br>Bridge/Tunnel<br>Tracks<br>Gauge<br>Embankment height<br>Service<br>Frequency |
| Ports | (Verschuur, Koks, et al., 2022) | Ports<br>Terminals | Area<br>Main use<br>Elevation |
| Inland Water Ways | UNECE, (2022) | Ports<br>Channels<br>Locks | Handling capacity<br>Max vessel dimensions<br>Width<br>Depth |
| Airports | OpenstreetMap | Main airports<br>Airfields | Contours<br>Buildings<br>Lanes |
| Intermodal terminals | Intermodal-map | Terminals | Number of modes<br>Number of cranes<br>Container bridge<br>Number of loading tracks<br>Length of loading tracks |

**Table 4:** Databases selected for the resources network analysis, as the basis of the interdependency analysis

| Resources | Source | Layers | Features |
|---|---|---|---|
| Electricity | OpenstreetMap<br>ENTSOE Transparency Platform | Generation plant<br>Substation<br>Transmission grid<br>Distribution grid | Voltage<br>Frequency<br>Number of Cables<br>Number of Wires<br>Operator |
| Telecom | OpenstreetMap | Communications tower<br>Mast | Elevation<br>Material |

This project has received funding from the European Union's Horizon Europe research and innovation programme under grant agreement No. 101093854

| | | | |
|---|---|---|---|
| | Infrastructure Connectivity Map (ITU) | Fiber cables<br>Internet Exchange Points | Slug<br>Metro area |
| Gas | SciGrid (Diettrich et al.)<br>OpenstreetMap<br>ENTSOE Transparency Platform | Pipes<br>Compressors<br>Entry<br>LNG<br>Storage<br>Wells | |

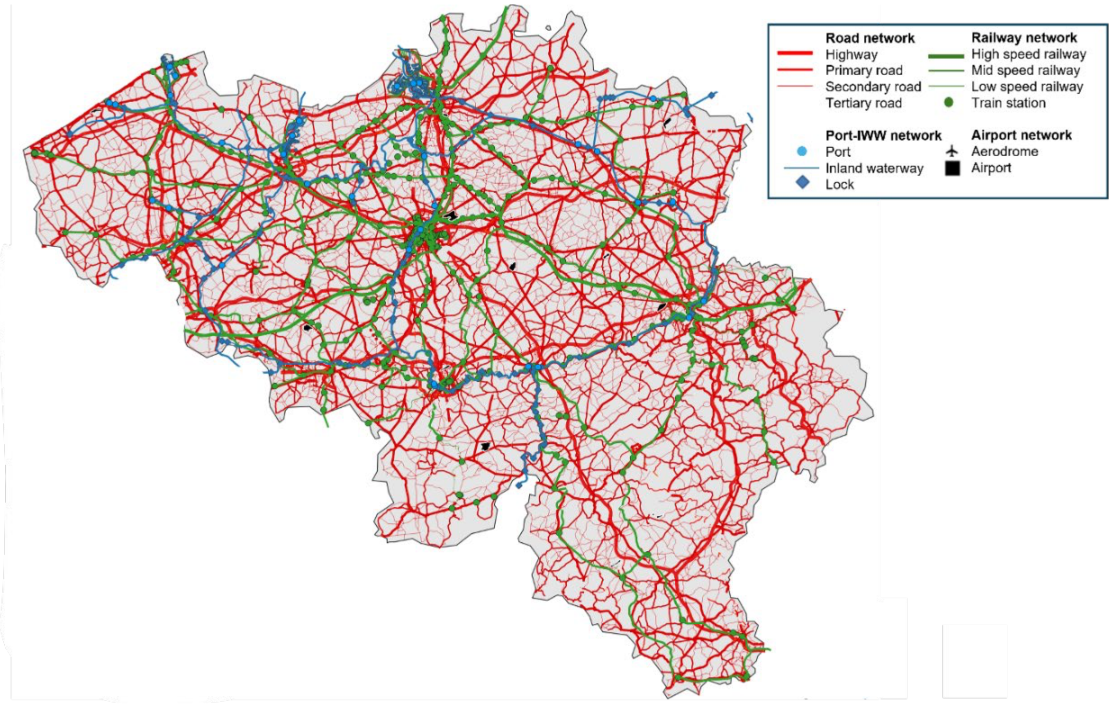


**Figure 9:** Visualization of the transportation networks datasets compiled for Belgium

This project has received funding from the European Union's Horizon Europe research and innovation programme under grant agreement No. 101093854

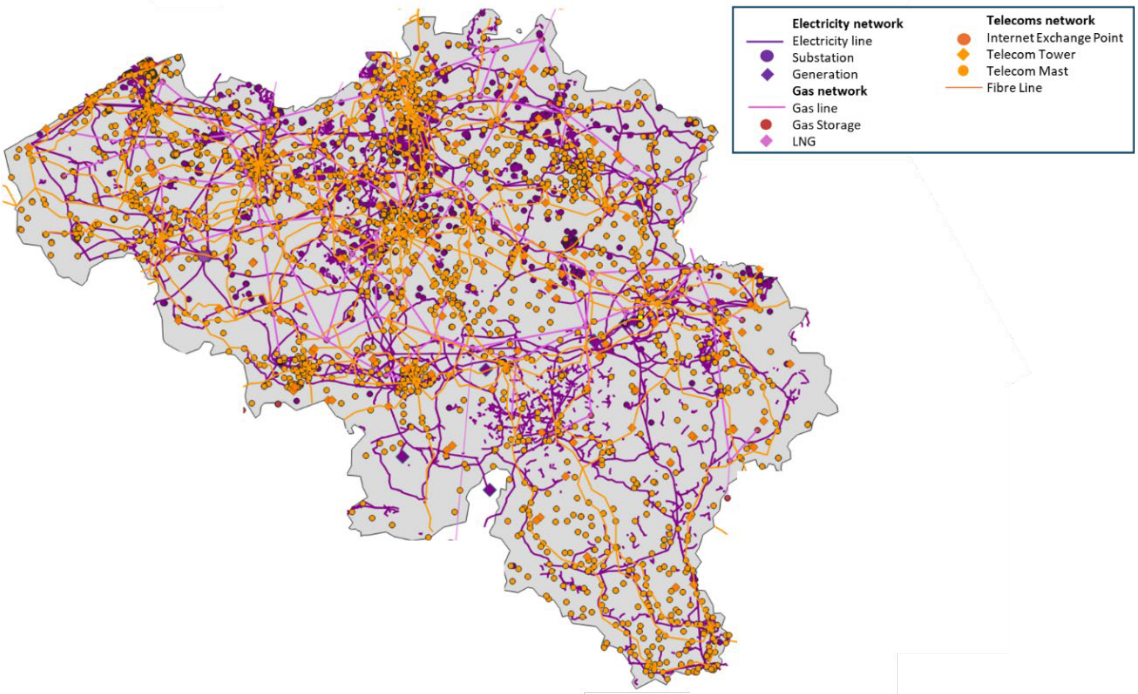


**Figure 10**: Visualization of resources networks datasets compiled for Belgium

This project has received funding from the European Union's Horizon Europe research and innovation programme under grant agreement No. 101093854

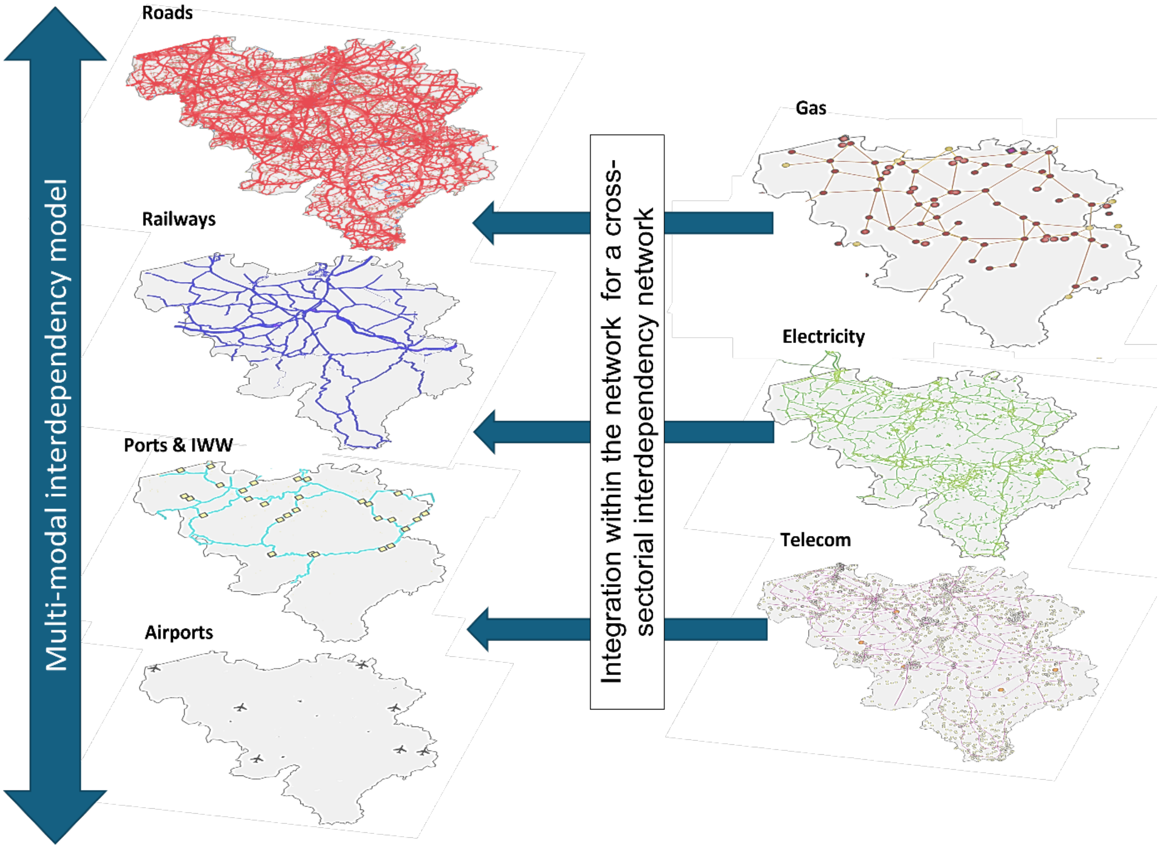


**Figure 11:** Integration of each mode and sector in the interdependency analysis for Belgium networks

## 3.2. Hierarchical resource networks

### Electricity network

Electricity networks in Europe are composed of interconnected infrastructure components that ensure the generation, transmission, and distribution of electrical power. These networks can be categorized into three hierarchical subsystems, corresponding to their functions and physical structure:

- Primary Network: The backbone of power generation and transmission. It includes large-scale power generation facilities such as coal, natural gas, nuclear, hydroelectric, wind, and solar plants. These plants generate electricity and feed it into the transmission network via step-up transformers that increase the voltage for long-distance transport.
- Secondary Network: This layer consists of high-capacity regional substations connected by long-distance transmission lines. These substations step down the voltage for regional distribution, acting as intermediary hubs that manage and control electricity flow to different parts of the grid.
- Tertiary Network: The final stage of electricity delivery. It involves local distribution transformers that step down the voltage further for safe use by

This project has received funding from the European Union's Horizon Europe research and innovation programme under grant agreement No. 101093854

residential, commercial, and industrial consumers. These transformers connect to the end users through lower-capacity distribution lines.

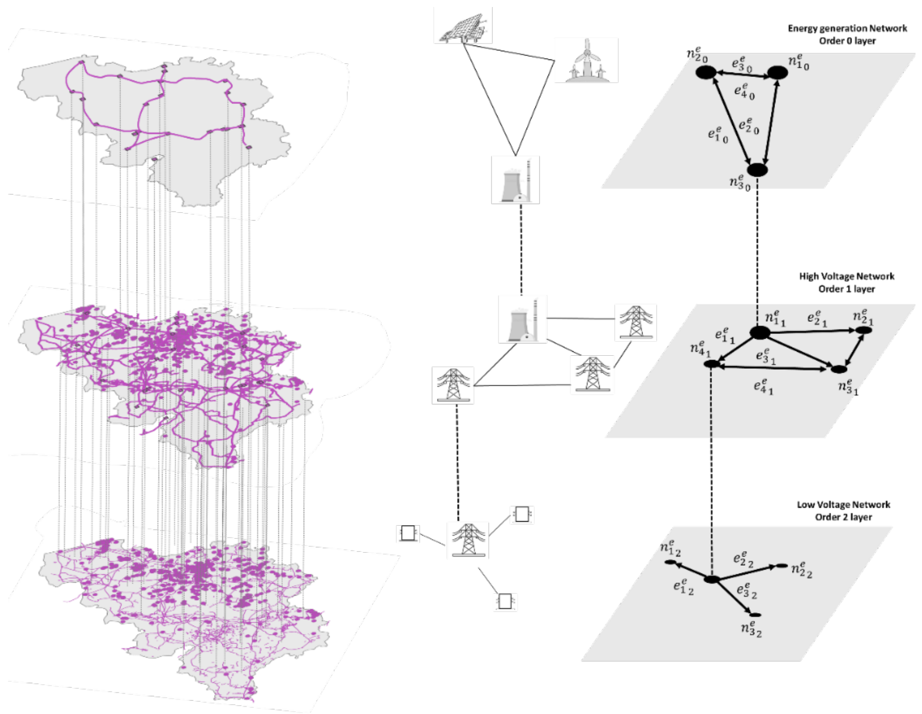


**Figure 12:** Topological representation of the different layers of the electricity network

## Natural gas network

The natural gas network in Europe is also typically organized into three hierarchical layers:

- Primary network: These are major infrastructure components, including gas storage terminals and extraction points, where gas is either stored or initially extracted from underground reservoirs. Primary nodes are essential for managing the availability and flow of gas across the entire network. These nodes often have large storage capacities and control the supply to the rest of the system.
- Secondary network: These are usually compressor stations, which help maintain the pressure and flow of gas within the pipeline system. Compressor stations play a crucial role in ensuring that gas moves efficiently over long distances by counteracting pressure losses that occur during transportation.
- Tertiary network: These represent the consumers of natural gas, including residential, commercial, and industrial users. At the tertiary level, natural gas is distributed to end users through local pipelines and pressure-regulated distribution networks.

This project has received funding from the European Union's Horizon Europe research and innovation programme under grant agreement No. 101093854

In this structured topology, primary nodes control the overall supply, secondary nodes manage flow and pressure, and tertiary nodes represent the final point of distribution. The hierarchy ensures that natural gas is efficiently transported from production sites to consumers, with each level playing a specialized role in the network's operation.

This tiered approach is essential for optimizing the flow of gas, responding to demand fluctuations, and ensuring the stability of the entire natural gas system.

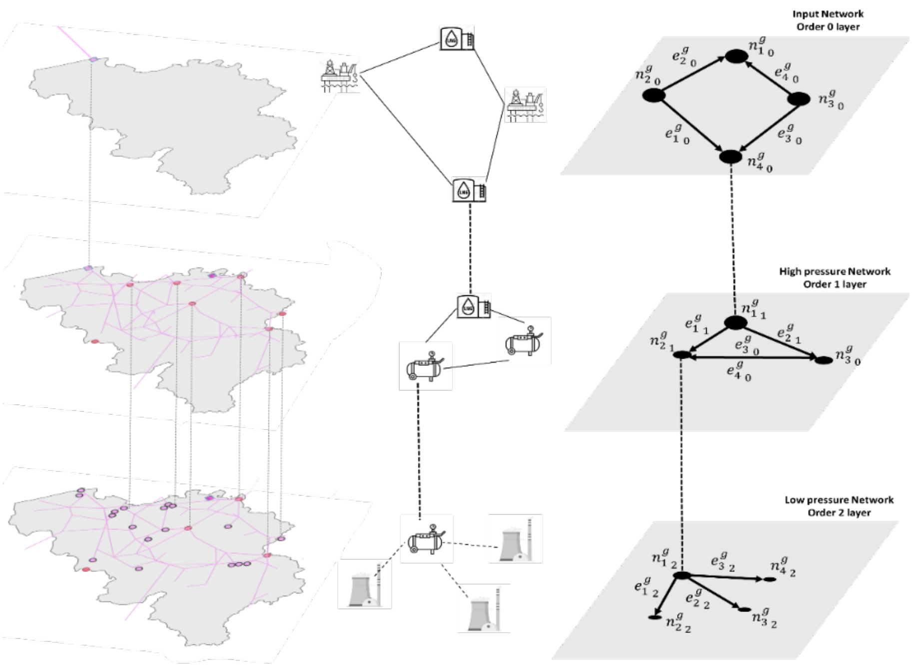


**Figure 13:** Topological representation of the different layers of the gas network

## Telecommunications network

Digital communications are categorized into three primary types of technologies: fixed networks (such as fiber, coaxial, and copper), wireless terrestrial networks (including cellular, Wi-Fi, and Tetra), and satellite networks (operating in geosynchronous, low Earth orbit, or medium Earth orbit). This analysis primarily focuses on the main fixed and wireless terrestrial networks, which can be modelled as the integration of three sub-systems (Pant et al., 2020).

- Core network: High-capacity long-distance connection network. It consists of fiber optic cables connecting a number of Internet Exchange Points at different countries.
- Internet Exchange network: Local access consisting of fixed fiber connecting the IEP with comms towers/macro-cells within same the region.

This project has received funding from the European Union's Horizon Europe research and innovation programme under grant agreement No. 101093854

- Cellular network: Wide-area macro cells, departing from the towers, as well as a smaller number of local-capacity small cells, departing from a number of comms masts.

In terms of connectivity, as depicted in Figure 14, Internet Exchange Points (IXPs) serve as direct links to the core internet (core network) and facilitate communication between IXPs within the same region. These connections rely on a robust network of fiber optic cables. Within the Internet Exchange Network, macro-cells are interconnected and linked to other sector assets through the same fiber optic infrastructure. Lastly, small cells, which are integral to the cellular network, connect to macro-cells via wireless links. Communication masts play a crucial role in this setup, acting as both receivers and distributors of wireless signals within each small cell's coverage area.

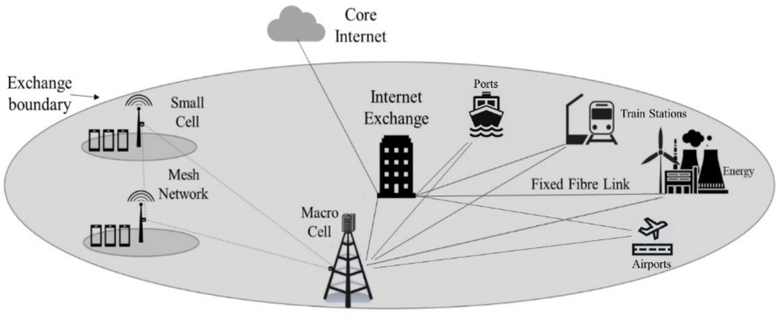


**Figure 14:** Schematic model of the telecommunications system (adapted from Pant et al. (2020))

The network architecture can be described as comprising three hierarchical layers: the core layer, is defined by the locations of Internet Exchange Points (IXPs) and the fiber optic cables that connect them, as per data from the ITU database. The topology of this layer consists of nodes (IXPs) interconnected by bidirectional edges, representing the two-way flow of data along the fiber network. The Internet Exchange Layer, which includes macro-cell towers identified in the OpenStreetMap database. These towers connect with one another and with the IXPs through the fiber optic cable network. The topology at this level features unidirectional edges (connecting IXPs to macro-cell towers, where data flows from the IXPs to the towers) and bidirectional edges (between macro-cell towers, enabling communication and redundancy). Additionally, macro-cell towers establish unidirectional connections to assets in other sectors, signifying the flow of information toward these assets. Finally, the cellular layer is defined by wireless connections between macro-cell towers and individual communication masts, as also documented in the OpenStreetMap database. These wireless connections are represented by unidirectional edges extending from macro-cell towers to the masts, which facilitate the distribution of data within each cell. This multi-layered structure ensures robust connectivity, with each layer playing a specific role in data transmission and network

This project has received funding from the European Union's Horizon Europe research and innovation programme under grant agreement No. 101093854

functionality. The hierarchical architecture and the topology are depicted in Figure 15.

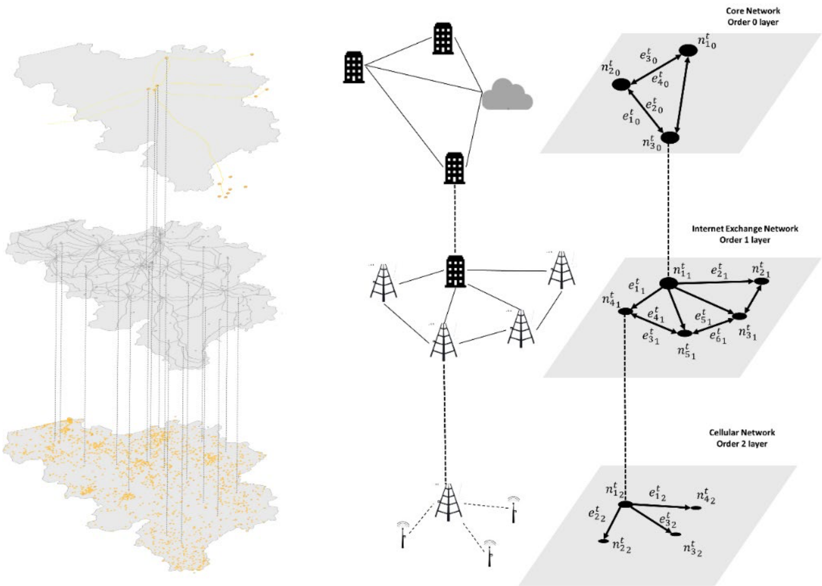


**Figure 15:** Topological representation of the different layers of the digital telecoms network

## 3.3. Transport Intermodal connectivity

Connectivity between different nodes is assumed to occur at specific, discrete locations within the network. For passenger transport, these points include train stations (rail-road connectivity), airports (rail-road-air connectivity), and ferry terminals (rail-road-water connectivity). For freight, connectivity is established at intermodal terminals, enabling transfers across rail-road, rail-air-road, and rail-water-road networks. These nodes serve as critical transfer points where flows of people and goods shift between networks, as illustrated in Figure 16.

From this figure, the structure of the multi-modal network topology becomes clear, showing how different mode-specific networks are interconnected through intermodal edges, $e_{ij}^{sl}$. These edges serve as conceptual links between modes at intermodal hubs—such as ports, airports, stations, and terminals. Importantly, these intermodal edges are not exact physical links but rather represent the physical co-locations where passengers or goods are transferred across modes.

To ensure the replicability of the methodology, asset-level notional nodes are used to assess the physical interconnections between different transportation modes. Figure 16 illustrates the asset-level locations of network connections. In ports (shown in blue in a) and airports (shown in black in b), rail (green lines) and road (red lines) network edges connect directly with the terminals, simplifying the distribution of flows. For land-based intermodal terminals (represented by orange hexagons in c and

This project has received funding from the European Union's Horizon Europe research and innovation programme under grant agreement No. 101093854

d), however, the chosen representation of road networks typically does not connect directly with terminal areas because they include only motorway, trunk, primary, secondary and tertiary roads and exclude more local roads. In these cases, secondary and tertiary links (yellow-circled branches) are designated as the entry/exit nodes for effective flow distribution.

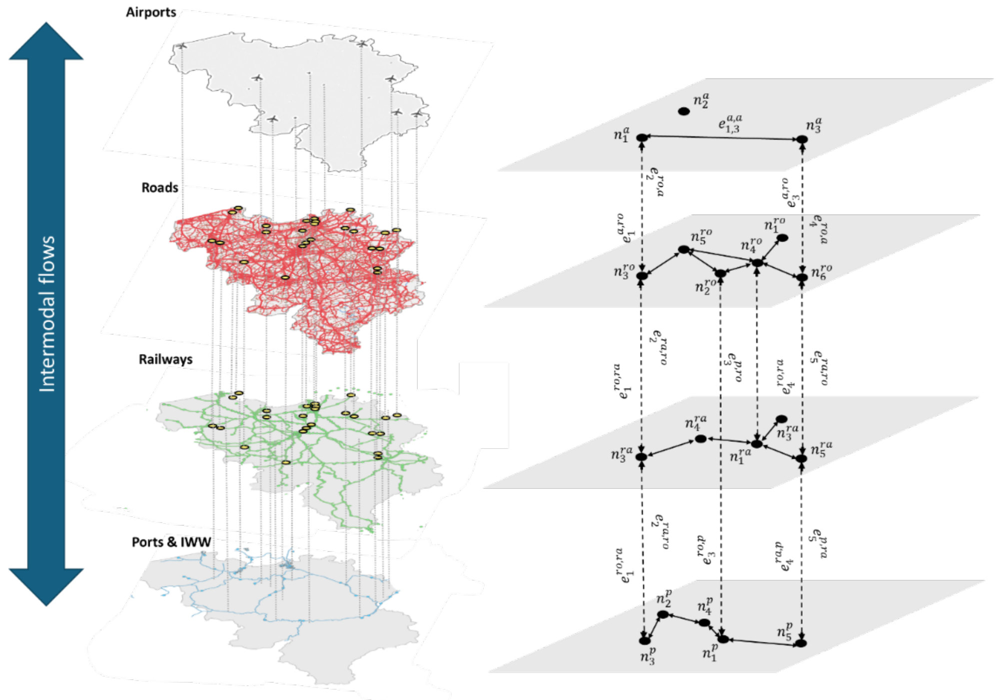


**Figure 16:** Intermodal connectivity and topological representation

(a) (b)

(c) (d)

This project has received funding from the European Union's Horizon Europe research and innovation programme under grant agreement No. 101093854

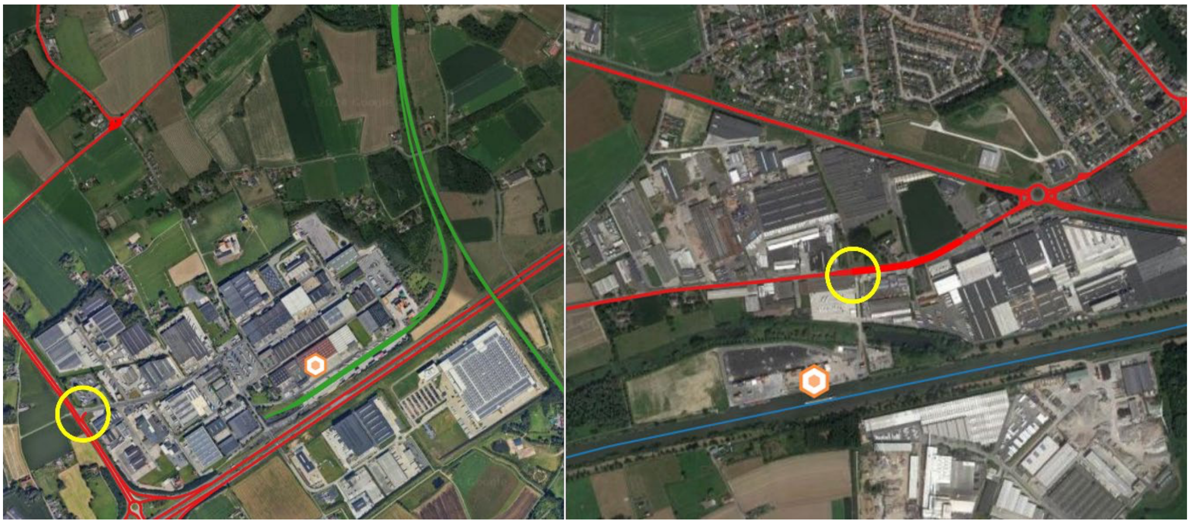

**Figure 17:** Intermodal terminals as connectors between transportation mode networks and topological representation

## 3.4. Operability dependency assessment

### Port, airport and intermodal terminals dependency on telecom and electricity networks

According to Table 2, ports and airports connect to substations rather than directly linking to power lines. Figure 18 illustrates an exploration of cross-sectorial connectivity: electricity and telecom networks connecting with port and airport terminals. In cases where there is an abundance of electricity lines and communication masts near shipping and storage terminals, establishing these links is determined by geographic co-location (left side of Figure 18). However, in scenarios with sparse connectivity (right side of Figure 18), assumptions must be made regarding both physical and notional connections between electricity networks and substations to maintain functional continuity. Consequently, this approach also involves assuming both physical and notional connections between substations and terminal points to support functional requirements, usually based on proximity (see red arrow in Figure 18). In terms of telecom connections, they are assumed to rely on masts, also based on proximity. Redundancy is assumed for masts, losing functionality when more than half of the nearest masts are disrupted.

This project has received funding from the European Union's Horizon Europe research and innovation programme under grant agreement No. 101093854

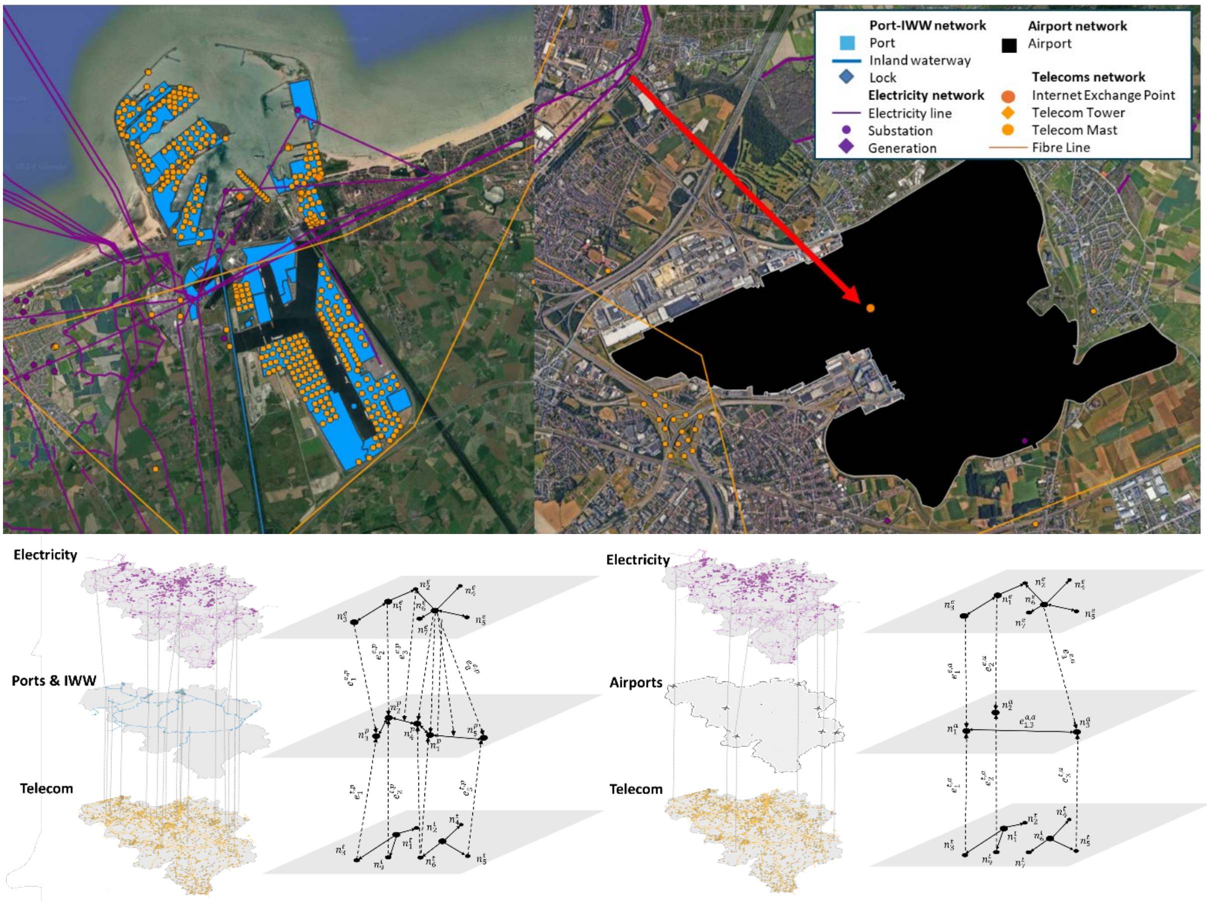


**Figure 18:** Operability links between electricity|telecom networks and port|airport terminals

The same approach extends to train stations and intermodal terminals, as illustrated in Figure 19. This figure also shows the notional connections required between the electricity network and inland waterway (IWW) locks, which are essential for operating lock mechanisms (opening and closing). These notional links ensure that all essential nodes—whether for rail, road, or waterway transport—maintain consistent operational support from the electrical grid, particularly in areas where direct physical connections may be limited.

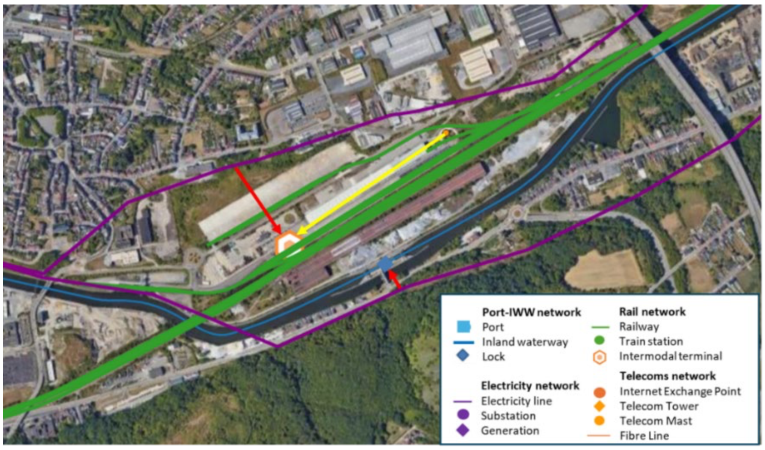


This project has received funding from the European Union's Horizon Europe research and innovation programme under grant agreement No. 101093854

Figure 19: Operability links between electricity (red arrows) / telecom (yellow arrows) networks, rail and intermodal terminals

### Road and railways dependency on telecom and electricity networks

Similarly, road and railway networks maintain operational links to the electricity network via low-voltage substation connections. For road networks, critical operational connections are only assumed in tunnel areas, where constant power is essential for ventilation, lighting, and safety systems (2004/54/EC). For railway segments, a spatial assignment method based on Voronoi polygons (illustrated as white lines in Figure 20) is employed. Each rail segment (shown as bold, colored lines) is assigned to the nearest available substation for electricity linkage and to the nearest telecom mast for communications. This method efficiently delineates service areas, ensuring that each rail segment has access to the essential infrastructure needed for operational continuity.

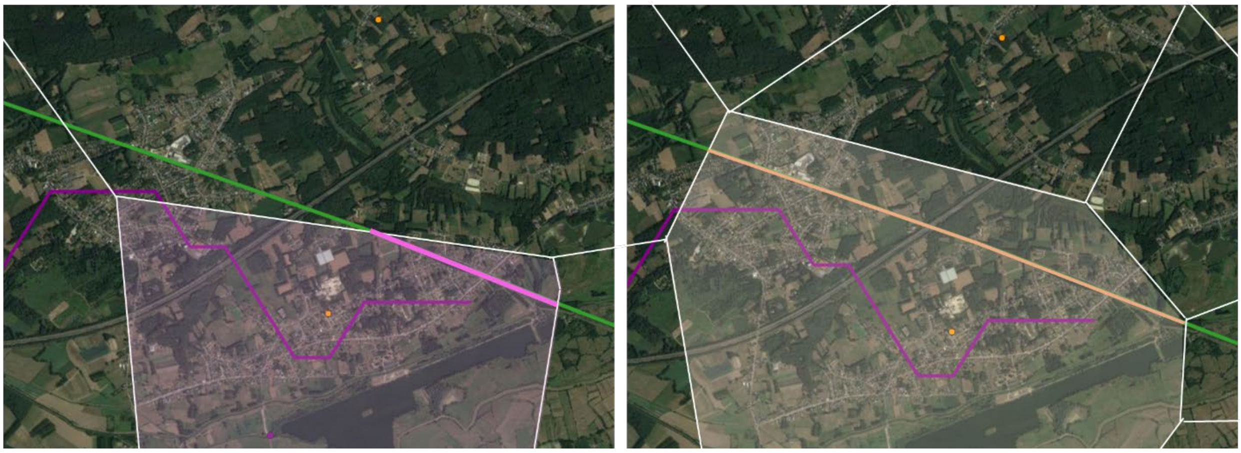

**Figure 20:** Railway segment assignment (based on Voronoi polygons) to define dependencies between railway, telecom and electricity networks

By utilizing Voronoi polygons to assign railway segments to the closest infrastructure resources, this approach optimizes connectivity and supports reliable, localized resource allocation across the network.

### Interdependencies between telecom, electricity and gas networks

The gas, electricity, and telecommunications networks are interdependent. The gas and electricity systems depend on each other in two main ways. First, thermal power plants rely on natural gas to generate electricity, which means they depend on the gas network. Second, the assets in the gas network, like storage tanks, pipelines, and LNG facilities, require electricity to operate.

As shown in , thermal power plants (generation nodes within the electricity network) incorporate consumer gas storage points, establishing a notional link between them. Additionally, point assets in the gas network (storage tanks, pipelines, and LNG terminals) are connected to the nearest substation to ensure the necessary power

This project has received funding from the European Union's Horizon Europe research and innovation programme under grant agreement No. 101093854

supply. For pipeline segments, similar to the method used for railway connections, Voronoi polygons are calculated around substations to designate the service area for each pipeline segment. This approach ensures that each section of the gas network is allocated to the closest substation, enabling efficient intermodal dependencies across network assets.

The telecom network's dependency on the electricity network primarily operates through each telecom mast's connection to the nearest electricity infrastructure, as illustrated in . It is also assumed that power stations and substations require telecom connectivity and are linked to the nearest telecom mast. In instances where multiple masts are in proximity, network resilience is factored in by assuming a loss of connectivity if more than half of the nearby masts are non-operational.

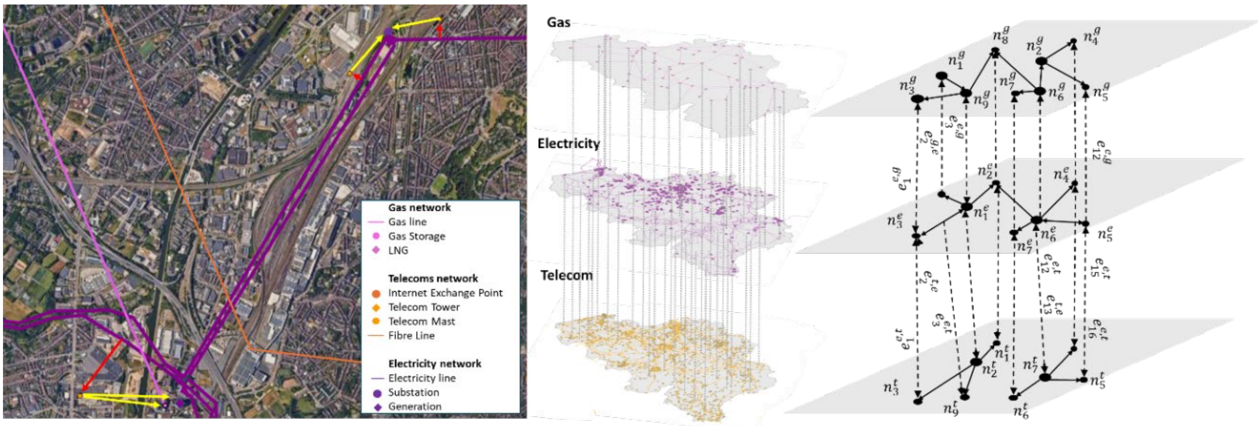


**Figure 21:** Interdependency links between gas, electricity, and telecom networks shown with the yellow arrows (from telecoms towards electricity/gas) and red arrows (from electricity towards telecoms).

## 3.5. Accessibility dependency assessment

Another type of dependency to consider is the accessibility of physical assets within infrastructure networks, particularly for enabling maintenance or repairs when disruptions occur. Ensuring access is essential in cases where, without intervention, a breakdown could worsen, leading to extended periods of non-operability or even triggering further disruptions across the network.

For this type of dependency, assets in the electricity, gas, and telecom networks are generally assumed to rely on road access. The premise is that if there is no functional road connection between the asset and a nearby main road, such as a motorway or highway, access cannot be assured. This road access dependency is visually represented in Figure 22, where reliable connectivity between energy and telecom assets and the primary road nodes (such as $\{n_4^{ro}\ and\ n_5^{ro}\}$ must be maintained. Maintaining these connections is essential to provide uninterrupted access for routine maintenance or emergency repairs. Consequently, a clear, functional link

This project has received funding from the European Union's Horizon Europe research and innovation programme under grant agreement No. 101093854

must be established between these critical assets and the main road network to ensure they remain accessible for necessary interventions.

This project has received funding from the European Union's Horizon Europe research and innovation programme under grant agreement No. 101093854

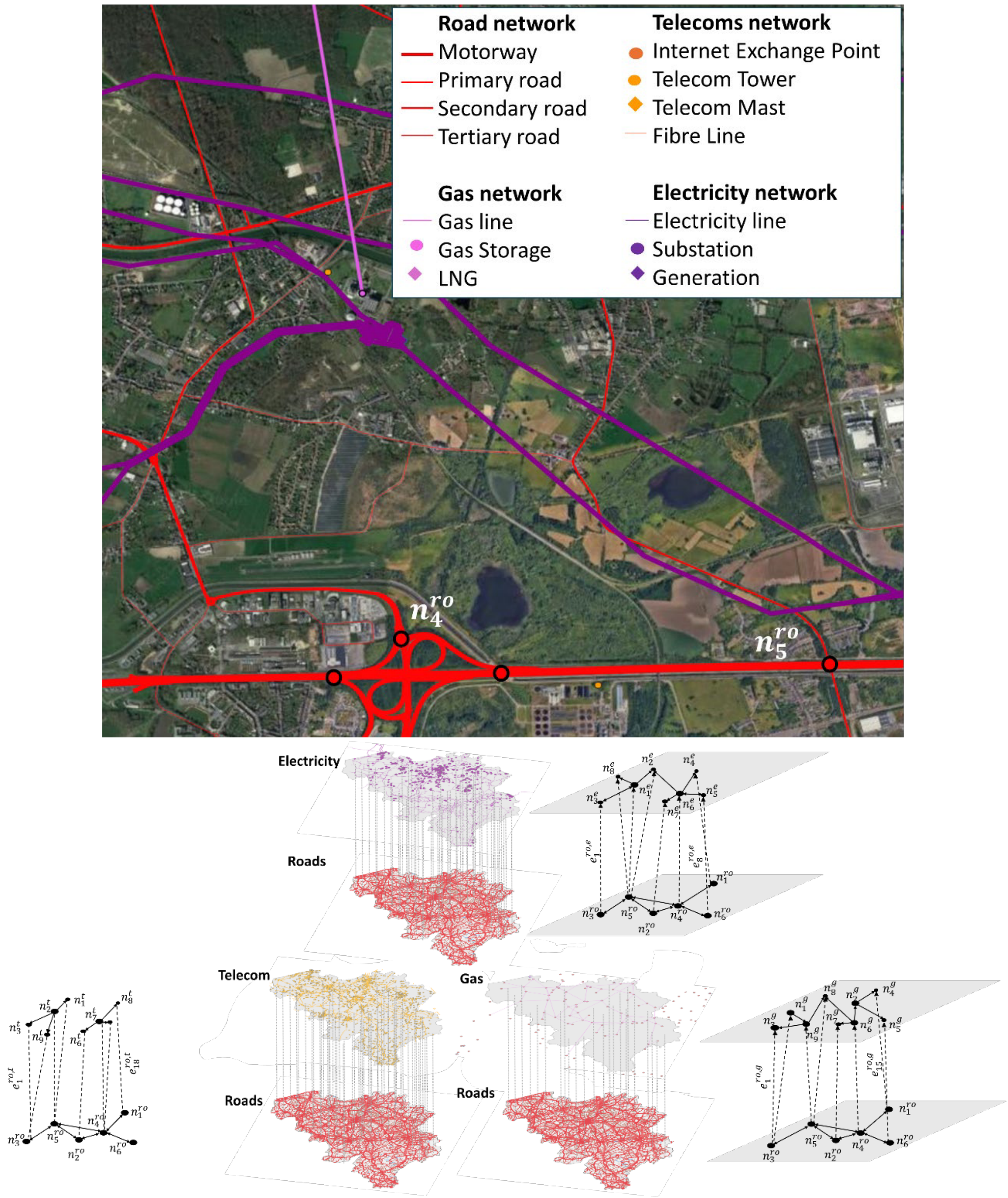


**Figure 22:** Accessibility links for the gas, telecom and electricity assets

This project has received funding from the European Union's Horizon Europe research and innovation programme under grant agreement No. 101093854

# 4. Network flow datasets and proposed model approaches

Network flow models are essential for mapping the failure propagation across networks. Here initial the proposed models for network flow modelling for different sectors in MIRACA are briefly discussed. It is noted that some of these models might undergo changes during their implementation phase (which follows Task 2.2 in Tasks 2.3 - 2.5 of MIRACA).

## 4.1. Pan-European flow databases

To analyze the transport, energy, and information (telecoms) flows between network nodes, Supply-Demand or Origin-Destination (OD) matrices are required as the primary input for the flow allocation model. Therefore, OD data must be gathered for the identified network nodes. However, as shown in Table 5, the homogeneity of the datasets is not guaranteed, with variations in data sources, types, and resolutions.

**Table 5:** Passenger, commodity and energy flow data for the transportation modes and resources to be explored

| Mode | Data source | Data description | Spatial resolution | Time resolution |
|---|---|---|---|---|
| Road | Eurostat | Commodity flow (by commodity) in/out flow from every region | NUTS3 | Annual |
| | ETIS (Speth et al., 2022) | Passenger and commodity flow between regions | NUTS3 | Annual |
| | E-Roads Census (UNECE, 2017) | AADT per main road | Road | Annual |
| Railway | Eurostat | Passenger and commodity flow between train stations | Railway | Annual |
| | Eurostat | Commodity transported, by cargo type, through each country | Country | Annual |
| | Eurostat | Passenger flow in/out flows | NUTS2 | Annual |
| | Eurostat | Commodity flow in/out flows | NUTS2 | Annual |
| | E-Rails Census (UNECE, 2017) | AADT per main railway | Railway | Annual |
| Airports | Eurostat | Passenger and commodity flow between airports | Airport | Annual |
| Ports | Eurostat | Passenger and commodity in/out flows from every port | Port | Quarterly |
| Inland water ways | Eurostat | Commodity in/out flows between every port | NUTS 2 | Quarterly |

This project has received funding from the European Union's Horizon Europe research and innovation programme under grant agreement No. 101093854

| | | | | |
|---|---|---|---|---|
| Electricity | ENTSOE Transparency Platform | Electricity production and consumption, technical parameters of national transmission networks (above 220 kV) | NA | Hourly |
| Gas | ENTSOG Transparency Platform | Electricity production and consumption, technical parameters of national transmission networks | NA | Hourly |

It is noted that for transport networks in many cases OD matrices for commodity and in some cases for passengers are available at high-level spatial resolutions. In cases where transport OD matrices are unavailable, population datasets will be used to generate the missing information. For energy networks (electricity and gas) there is no available information on any type of OD matrix that would be in the form of the supply and demand values at nodes or aggregated scales. For such sectors process flow models with relevant network attributes would help create an OD matrix through optimizing the process of supply and demand balance. For telecoms there is no data on service provided by assets, and hence population datasets could be used to map services between source and sink nodes to create an OD matrix.

## 4.2. Transportation flow models

For each of the transportation mode, the flow allocation (for passengers and commodity) model will vary depending on the data availability.

### Roadways

#### *General flow allocation model*

For roads, the flow allocation uses a modified model for passengers and commodity based on the work by Li et al. (in preparation). The flow allocation model is used to distribute the flows between all the edges that connect any pair of nodes from the matrix. The model involves the following iterative steps:

- Identification of OD-nodes, edges, and flows: For each node pair, flows are extracted from the Origin-Destination (OD) matrices, and edges are defined by connectivity (from-to nodes).
- Initialization: Flows are assigned based on the shortest paths between nodes. To calculate the shortest path, a cost function $c_{ij}$, which is applied for each edge:

$$c_{ij} = VoT\ t_{ij} + b_{ij} + d_{ij} \quad [6]$$

Where $VoT$ is the value of time (in euros/hour) for passengers or goods, $t_{ij}$ is the travel time (based on flow velocity and edge length $t_{ij} = \frac{l_{ij}}{v(q_{ij})}$), $b_{ij}$ represents toll costs, and $d_{ij}$ accounts for customs costs. Flow velocity depends on the assigned flow $q_{ij}$ and the remaining road capacity.

This project has received funding from the European Union's Horizon Europe research and innovation programme under grant agreement No. 101093854

- Flow adjustment: To prevent overflows, a flow adjustment ratio is computed:

$$r(k) = \min_{k}\left(\frac{C_{ij}(k-1)}{q_{ij}(k)}\right) \quad [7]$$

Where $C_{ij}(k-1)$ is the remaining edge capacity from the previous iteration $(k-1)$, and $q_{ij}(k)$ is the flow assigned in the current iteration $(k)$. This ratio is applied to adjust flows and avoid overflows.
- Network update: Flow velocities and remaining capacities are updated. If flows remain unassigned, the iteration repeats.

The overall workflow is depicted in Figure 23. To distribute the flows effectively, it is necessary to compute the Origin-Destination (OD) matrices between road nodes, as direct data for passenger and commodity cargo flows at a pan-European scale is not readily available. Distinct approaches are employed to derive the OD matrices for passenger flows and commodity flows, tailored to their specific characteristics and requirements.

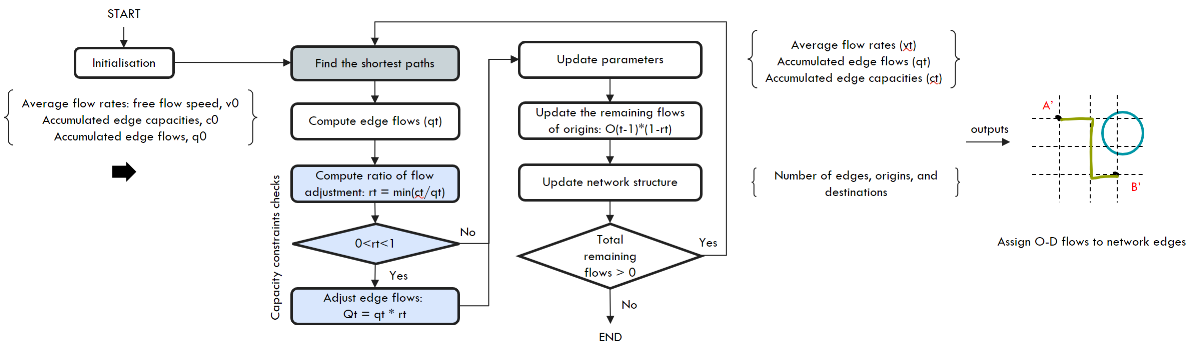


**Figure 23:** Flow allocation model for the road network

### *Passenger flows*

For passengers, population data is used to estimate how many people travel through each node. A Voronoi polygon is drawn around each node, and the flow is assigned based on the population inside each polygon. The population data comes from the GHS database (European Commission, 2023). Then, a "radiation model" (Masucci et al., 2013) is used to further distribute the flow between any two nodes in the network.

$$F_{ij} = F_i \frac{m_i n_j}{[(m_i+s_{ij})(m_i+n_j+s_{ij})]} \frac{1}{1-\frac{m_i}{\sum m_i}} \quad [8]$$

Being $F_i$ the origin node outgoing flow, $m_i$ the origin population, $n_j$ the destination population, $s_{ij}$ the population in a circle whose center is the origin and radius the distance between the origin and the destination, minus the population at the origin and the population at the destination. In simple terms, this model uses population distribution to estimate how passenger flows move between nodes, and then adjusts these flows using the radiation model equation.

This project has received funding from the European Union's Horizon Europe research and innovation programme under grant agreement No. 101093854

*Commodity flows*

For commodity flow distribution, economic activity (based on industries' location) is used as the main distribution factor. Industries are classified by type (based on an aggregated NST07), and commodity is distributed to those locations based on Input-Output theory (Leontief, 1951). The distribution procedure is based on the assumption that each industry produces a specific type of commodities (NST07) (see Table 6 below), but the inputs required to produce these commodities may vary. As a result, the OD (origin-destination) matrix for each industry may include different commodities based on the final products of the destination industry location. To obtain the asset specific (node level) OD matrices, the different commodities flowing from the origin region to the destiny industry are computed via:

$$F_{ij\,NUTS2_{GTX}} = \left(I - A'_{ij}\right)^{-1} P_{GTX_j} \quad [9]$$

Where $F_{ij\,NUTS2_{GTX}}$ is the flow of commodities, that come from the origin region (i), necessary for production at the destiny industry ($P_{GTX_j}$) and $A'_{ij}$ is the Input-Output matrix between origin (i) and destination (j) regions, modified to account for tons production. To be noted, production and flows within the same region are also computed, but in this case $A'_{ij}$ is the IO matrix for the same region.

The final OD flow is downscaled proportionally to the industry locations at the origin region:

$$F_{ij_{GTX}} = F_{ij\,NUTS2_{GTX}} \frac{P_{GTX_i}}{\sum_{NUTS2} P_{GTX_i}} \quad [10]$$

Being $F_{ij_{GTX}}$ the OD flow for a given industry sector (by commodity), $F_{ij_{NUTS2_{GTX}}}$ the OD flow for the NUTS2 region for a given commodity, $P_{GTX_j}$ the production output of a given industry for a given commodity and $\sum_{GT} P_{GTX_{j_{NUTS2}}}$ the sum of outputs of all industries of the destiny NUTS2 region. This method ensures that commodity flows are proportionally assigned to industry locations based on output.

The methodology is illustrated in Figure 24. As a general rule, nodes that are not linked to a specific industry location are excluded from the initial flow assignments. These nodes will only be populated with flow data once the allocation process for the edges has been completed.

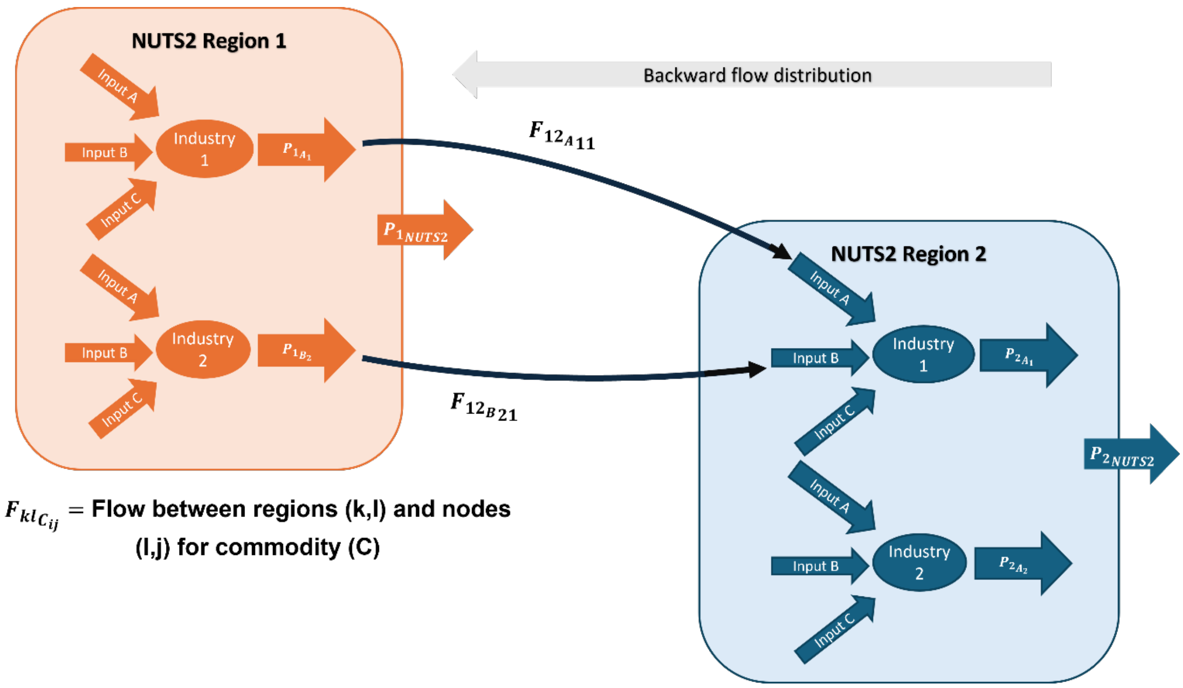


**Figure 24:** Diagram of OD matrices computation for the industry specific nodes

*Vehicle flow distribution*

After the downscaling process of passenger and commodity OD matrices to specific locations, the flow allocation model is used to compute the edge flows described above. This model serves to allocate vehicle flows in the edges based on vehicle OD matrices. Passenger and commodity flows are then converted to car and truck flows based on the assumptions outlined in Table 6. The table provides average values for European countries, though specific values were calculated for each country and NST07 cargo type using EUROSTAT data. These assumptions help refine the flow distribution, ensuring it reflects the particular transportation needs and capacities of each region.

**Table 6: Road vehicles' occupancy rate for passenger traffic and each type of cargo (commodity)**

| Cargo type | Cargo/vehicle (μ) | Coef. of variation (σ/μ) |
|---|---|---|
| Passengers | 1.15 [passengers/trip] | 6.15% |
| GT1 (Agriculture products) | 15.98 [tons/trip] | 6.36% |
| GT2 (Coal, oil and gas) | 15.83 [tons/trip] | 3.22% |
| GT3 (Mining products) | 18.42 [tons/trip] | 5.00% |
| GT4 (Food products) | 13.10 [tons/trip] | 3.05% |
| GT5 (Textiles) | 6.97 [tons/trip] | 1.75% |
| GT6 (Wood) | 13.17 [tons/trip] | 2.59% |
| GT7 (Coke and petroleum) | 17.92 [tons/trip] | 3.88% |
| GT8 (Chemicals) | 14.22 [tons/trip] | 2.44% |

This project has received funding from the European Union's Horizon Europe research and innovation programme under grant agreement No. 101093854

| | | |
|---|---|---|
| GT9 (Other minerals) | 14.42 [tons/trip] | 2.46% |
| GT10 (Fabricated metals) | 12.10 [tons/trip] | 2.95% |
| GT11 (Machinery & Equip.) | 9.28 [tons/trip] | 2.00% |
| GT12 (Transport equip.) | 9.60 [tons/trip] | 2.81% |
| GT13 (Furniture) | 8.24 [tons/trip] | 3.18% |
| GT14 (Secondary raw) | 10.63 [tons/trip] | 2.51% |
| GT15 (Mail) | 8.84 [tons/trip] | 2.97% |
| GT16 (Transport material) | 3.52 [tons/trip] | 0.46% |
| GT17 (Baggage) | 6.87 [tons/trip] | 1.75% |
| GT18 (Grouped goods) | 11.71 [tons/trip] | 2.04% |
| GT19 (Unidentifiable) | 13.71 [tons/trip] | 8.41% |
| GT 20 (Other) | 13.07 [tons/trip] | 4.35% |

Vehicle flows, including both cars and trucks, are systematically allocated to each node using a structured approach to ensure accuracy and consistency. The assignment of cars begins by taking the passenger values from the Origin-Destination (OD) matrix. Each value is divided by a number randomly selected from a normal distribution $N(\mu,\sigma)$ reflecting the variability in passenger transport.

For truck flows, the process is slightly different as it accounts for the type of commodity being transported. The commodity values from the OD matrix are divided by a similar number chosen from each commodity normal distribution $N(\mu,\sigma)$. This distinction allows for a more precise allocation of trucks based on specific cargo types. Once the truck flows are established, they must be converted into an equivalent passenger car flow. This conversion utilizes the Passenger Car Equivalent (PCE) method, as recommended by the European Commission, which assigns a PCE value ranging from 2 to 3 based on varying road conditions. To refine this conversion, the PCE adjustment is made using a normal distribution $N(2.5,0.7)$, ensuring that the final truck flow representation reflects a more precise equivalency in terms of passenger car flows.

Once the calculations for both cars and trucks are completed, the results are aggregated into a homogeneous OD vehicle matrix. This matrix facilitates a comprehensive understanding of vehicle flows at each node, enabling effective transportation planning and management. By employing this methodology, we ensure that the distribution of vehicle flows accurately represents real-world conditions.

The next step involves flow allocation based on the outlined methodology, incorporating the combined flows of cars and trucks (). Notably, the maximum capacity of each edge is taken into account during the allocation process. This

This project has received funding from the European Union's Horizon Europe research and innovation programme under grant agreement No. 101093854

capacity represents a joint maximum limit, reflecting the combined flows of trucks and cars.

*Passenger and commodity flow distribution*

After determining the total vehicle flows, it is crucial to differentiate between passenger cars and trucks to derive the final passenger and commodity flows (measured in tons by cargo type) for each edge. This process involves reallocating the total flows into their respective passenger and commodity components. The redistribution is performed by proportionally assigning the vehicle flows to the outgoing flows from the origin node.

$$F_{cars\,k} = F_k \frac{F_{cars\,i}}{F_{cars\,i}+PCE\,[T_{GT1_i}+T_{GT2_i}+\cdots+T_{GT20_i}]} \qquad [11]$$

$$F_{trucks\,GTX\,k} = F_k \frac{F_{trucks\,GTX\,i}}{F_{cars\,i}+PCE\,[F_{trucks\,GT1_i}+F_{trucks\,GT2_i}+\cdots+F_{trucks\,GT20_i}]} \qquad [12]$$

In these equations, $F_{cars\,k}$ denotes the number of cars traversing the edge, while $F_{trucks\,GTX\,k}$ represents the number of trucks transporting commodity type GTX along the same edge. Here, $F_k$ signifies the total number of vehicles on the edge, as determined by the flow allocation model. $F_{cars\,i}$ indicates the number of cars departing from the origin node, and $F_{trucks\,GTX\,i}$ reflects the number of trucks carrying commodity type GTX departing from the origin node.

By employing this methodological approach, we achieve a thorough flow distribution across all edges in the network, thereby effectively differentiating between passenger vehicle flows and commodity flows corresponding to each specific type of cargo.

## Railways

For railways, a Eurostat provides data that includes OD matrices for the main stations in each country, distinguishing between passenger and commodity trains (as listed in Table 5). The first step involves converting the data, originally expressed in terms of train trips, into commodity volumes (in tons by NTS07 type of goods) and passenger volumes. Since data on trains per cargo type is unavailable, assumptions from Table 7 and Table 8 are applied. For each train trip, a maximum capacity and occupancy rate are sampled from corresponding distributions, assigning flows to each edge for passenger and commodity trains separately.

Commodity train trips are not initially broken down by cargo type. To address this, a node-specific distribution factor for cargo types is calculated (cargo volume for each type relative to the total cargo volume). To obtain these factors, firstly each industry facility output is assigned to a commodity train station based on the lowest

This project has received funding from the European Union's Horizon Europe research and innovation programme under grant agreement No. 101093854

cost function (lowest travel time) obtained from the road flow allocation model. Then, the flowing cargo is computed per cargo type based on:

$$F_{ij_{GTX}} = F_{ij} \left( \frac{P_{GTX_k}}{\sum_{GT} P_{GTX_k}} \right) \quad [13]$$

Being $F_{ij}$ the total cargo flow between stations, $P_{GTX_k}$ the cargo output (for the evaluated commodity) for all industries assigned to that station and $\sum_{GT} P_{GTX_k}$ the sum of cargo outputs of all commodities assigned to the station. This factor is then applied to each commodity trip, ensuring an accurate distribution of commodity by type across the railway network.

**Table 7:** Trains' capacity and occupancy rates for passenger trains (European Environment Agency, 2000; TRUST,2024)

| Train type | Train capacity (passenger/train) | | Occupancy rate | |
|---|---|---|---|---|
| | μ | σ/μ | μ | σ/μ |
| Regional, short distance | 200 | 5% | 0.4 | 10% |
| Regional, long distance | 400 | 5% | 0.5 | 10% |
| Interregional, high speed | 500 | 5% | 0.7 | 10% |

**Table 8:** Trains' capacity and occupancy rates for commodity trains (European Environment Agency, 2000; TRUST,2024)

| Train type | Train capacity (tons/train) | | Occupancy rate | |
|---|---|---|---|---|
| | μ | σ/μ | μ | σ/μ |
| Intermodal | 700 | 5% | 0.9 | 10% |
| Bulk, short distance | 700 | 5% | | |
| Bulk, long distance | 1500 | 5% | | |

However, the database does not account for cross-border transportation between stations in different countries. To address this gap, the OD matrices of commodity and passenger flows between NUTS-2 regions are used. It is assumed that for traffic between NUTS-2 regions in different countries, the flows are assigned to the nearest outgoing or incoming railway stations within the respective regions. This ensures that international railway traffic is accurately reflected in the model. The initial OD matrices have been successfully transformed into a flow database, representing edge-level flows across the pan-European network. The final step is to calculate each edge's maximum capacity, ensuring that no edge reaches or exceeds its maximum

This project has received funding from the European Union's Horizon Europe research and innovation programme under grant agreement No. 101093854

train flow. The maximum daily train capacity for each edge ($k \equiv ij$) is determined using the following formula:

$$C_k = \frac{V_{f_k}}{D_k} OT_f + \frac{V_{p_k}}{D_k} OT_p \qquad [14]$$

where $C_k$ represents the maximum daily train capacity on edge, $V_{f_k}$ is the commodity train speed on edge $V_{p_k}$ is the passenger train speed on edge $OT_f$ denotes the operational time for commodity trains (24 hours), and $OT_p$ denotes the operational time for passenger trains (18 hours). $D_k$ is the travel distance in the edge. This calculation ensures that each edge has a capacity that accommodates the anticipated train flow, optimizing network performance and minimizing congestion risks.

### Airports

For airports, Eurostat provides detailed passenger and commodity data between major airports (national, European, and international), therefore the OD-matrices (see Table 5). Flow allocation is straightforward since only the maximum node capacity needs consideration, not edge capacity. Node capacity is determined by the maximum number of available aircrafts per airport (EUROSTAT) and the number of runways. Similar to the road allocation model, a linear flow reduction function is applied to each node, accounting for both regular and maximum capacities. This ensures that as airports approach their capacity limits, flows are adjusted accordingly to reflect potential congestion and operational limits, optimizing the overall flow distribution.

$$C_i = \frac{\sum Ac_j Cap_j}{\sum Ac_j} \left[ \frac{N_{lanes}}{2} G \frac{operable\ hours}{year} L_{cap} \right] \qquad [15]$$

Let $Ac_j$ represent the aircraft (by type) at a given airport, and $Cap_j$ denote the tonnage or passenger capacity of each aircraft. The number of lanes, $N_{lanes}$ , is divided by 2, as runways typically operate in parallel (2-by-2). The lane capacity is assumed to be 10 aircraft per lane per hour. $G$ represents the total number of operable hours in a year (18 hour/day and 365 days/year). Thus, the total capacity of the airport can be estimated by considering the aircraft type, its capacity, and the runway throughput, providing a comprehensive view of the airport's operational limits.

### Ports and inland waterways

For maritime ports, their OD-matrices are also obtained from a global shipping model, which estimates port capacities in tonnages consistently (Verschuur et al., 2022).

This project has received funding from the European Union's Horizon Europe research and innovation programme under grant agreement No. 101093854

Finally, for inland waterways, the Eurostat data (loaded/unloaded commodity by port and shipped cargo by NUTS2 region) enables the distribution of commodity flows. Firstly, the distance between inland ports is computed by means of the channel length to be navigated. Then, the flow is computed assuming the cost function is depending on the navigating time.

$$F_{ij_{GTX}} = \frac{F_{ij_{NUTS2}GTX}}{\left(\frac{L_{ij}}{\sum L_{ij_{NUTS2}}}\right)} \quad [16]$$

Being $F_{IJ_{GTX}}$ the flow (by commodity type) between $ij_{NUTS2}$ regions, $F_{ij_{GTX}}$ the flow (by commodity type) between *i,j* ports, $L_{ij}$ the distance between ports and $\sum L_{ij_{NUTS2}}$ the sum of distance between all ports on those regions. Finally, flows within NUTS2 regions are computed based on the loaded/unloaded commodity by port.

## 4.3. Multi-modal transportation network analysis

### Intermodal flow allocation

Passenger and commodity-specific commodity flows will be allocated at intermodal nodes, based on the assumption that incoming and outgoing flows enter and exit through the closest available network node to each terminal. This allocation strategy is grounded in assumptions about the connectivity between transportation modes (explained in Chapter 3), ensuring both realistic and efficient flow distribution. Flow allocation across various transportation modes presumes that intermodal points—such as ports, airports, train stations, and intermodal terminals—act as hubs where different mode-specific flows converge, attracting and repelling these flows similarly to the industrial nodes in unimodal flow allocation processes.

In this framework, known air, maritime, and rail flows at terminal points enable the calculation of corresponding road transport flows, which are derived to balance the total passenger and cargo movements at each intermodal point. This ensures an accurate representation of mode transitions by passenger type and cargo type.

To support this intermodal connectivity, in the road NUTS2-level to asset level downscaling, intermodal points flow will function as constrains (as values in the origin-destination (OD) matrices). By anchoring road flow calculations to these reference nodes—which reflect the OD patterns captured at the NUTS3 level—the

This project has received funding from the European Union's Horizon Europe research and innovation programme under grant agreement No. 101093854

methodology enables a transition from broader regional data to precise asset-level flows.

The final road OD flow is downscaled proportionally to the intermodal locations at the origin region, updating Eq 13 into:

- For the industries

$$F_{ij_{GTX}} = F_{ij\,NUTS2_{GTX}} \frac{P_{GTX\,j}}{\sum_{NUTS2}\left[P_{GTX\,j} + F_{j\,NET\,T_{GTX}} + F_{j\,NET\,A_{GTX}} + F_{j\,NET\,W_{GTX}}\right]} \qquad [17]$$

- For the intermodal points

$$F_{ij_{GTX}} = F_{ij\,NUTS2_{GTX}} \frac{F_{j\,NET\,T_{GTX}} + F_{j\,NET\,A_{GTX}} + F_{j\,NET\,W_{GTX}}}{\sum_{NUTS2}\left[P_{GTX\,j} + F_{j\,NET\,T_{GTX}} + F_{j\,NET\,A_{GTX}} + F_{j\,NET\,W_{GTX}}\right]} \qquad [18]$$

Being $F_{ij_{GTX}}$ the OD flow for a given destination (j) intermodal point, $F_{ij_{NUTS2_{GTX}}}$ the OD flow for the NUTS2 region for a given commodity, $F_{j_{NET\,T_{GTX_i}}}$ the net flow (input-ouput) for a given mode (T, train, A, air and W, maritime) and $P_{GTX_j}$ the output of the industry. $\sum_{NUTS2}\left[P_{GTX_i} + F_{j_{NET\,T_{GTX_i}}} + F_{j_{NET\,A_{GTX_i}}} + F_{j_{NET\,W_{GTX_i}}}\right]$ is the sum of outputs of all industries of the origin NUTS2 region. This method ensures that commodity flows are proportionally assigned to industry locations based on output.

## 4.4. Resources network analysis

Resource networks such as electricity, telecommunications, and gas systems are critical for maintaining the functionality of transportation and infrastructure. Disruptions in these systems can propagate across sectors, causing cascading failures. This analysis models the topology, dependencies, and resilience of these systems by mapping network structures, evaluating the impacts of disruptions, and deriving resilience metrics.

### Electricity network

Electricity flow allocation models play a critical role in understanding and managing power distribution across the grid under various operational conditions. These models depend on accurate data and mathematical representations of physical laws to ensure efficient and reliable operation. Key data inputs include:

- Generation and load data: Collected at substations or aggregated at nodal or regional levels.

This project has received funding from the European Union's Horizon Europe research and innovation programme under grant agreement No. 101093854

- Transmission network data: Includes line parameters (impedance, susceptance) and transformer characteristics.
- Topology: Information about the connectivity and operational states (e.g., line outages, transformer tap settings).

Flow allocation models are based on fundamental laws of electricity (Wood et al., 2013):

- Ohms's law: Describes the relationship between voltage (*V*), current (*I*), and resistance (*R*)

$$V = I \cdot R \tag{19}$$

- Kirchhoff's Current Law (KCL): Ensures the sum of currents entering and leaving a node equals zero.

$$\sum_{k=1}^{N} I_k = 0 \tag{20}$$

- Kirchhoff's Voltage Law (KVL): Ensures the sum of voltages in a closed loop equals zero.

$$\sum_{k=1}^{M} V_k = 0 \tag{21}$$

These equations are solved iteratively in power flow calculations, using models such as the PI model, which represents network elements with series impedance (*Z*) and shunt admittance (*Y*), as depicted in Figure 25.

$$Z = R + j \cdot X \tag{22}$$
$$Y = G + j \cdot B \tag{23}$$

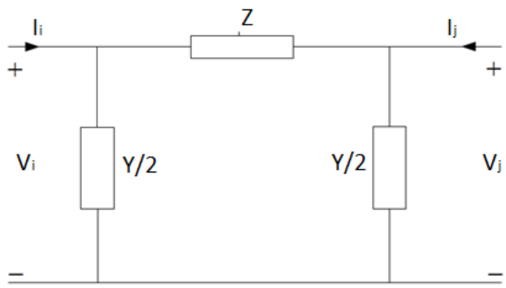


**Figure 25:** PI model of the network element

The flow allocation is based on power flow models (G. W. Stagg & A. H. El-Abiad, 1968; Grainger & Stevenson, 1994):

- Alternating Current (AC) Power Flow Model: Captures detailed operational aspects by solving nonlinear equations for active ($P_i$) and reactive ($Q_i$) power injections:

This project has received funding from the European Union's Horizon Europe research and innovation programme under grant agreement No. 101093854

$$P_i = \sum_{j=1}^{N} V_i \cdot V_j \cdot \left(G_{ij} \cdot \cos(\theta_i - \theta_j) + B_{ij} \cdot \sin(\theta_i - \theta_j)\right) \quad [24]$$
$$Q_i = \sum_{j=1}^{N} V_i \cdot V_j \cdot \left(G_{ij} \cdot \sin(\theta_i - \theta_j) - B_{ij} \cdot \cos(\theta_i - \theta_j)\right) \quad [25]$$

Where $\{G_{ij},\ B_{ij}\}$ are the conductance and susceptance of the line connecting nodes *i* and *j* and $\{\theta_i, \theta_j\}$ are the voltage angles at nodes *i* and *j*, respectively.

- Direct Current (DC) Power Flow Model: A linear approximation that ignores reactive power and assumes small voltage angle differences. It assumes constant voltage magnitudes, small angle differences between nodes and no reactive power and power losses.

$$P_{ij} = B_{ij} \cdot (\theta_i - \theta_j) \quad [26]$$

where $P_{ij}$ is the active power flow between nodes, and $B_{ij}$ is the line susceptance. This model is computationally efficient and widely used for large-scale applications like market clearing and contingency analysis.

Electricity flow is then distributed across the network based on impedance or admittance values, following a systematic allocation process (Kundur, 1994):
- Initial Power Injection: Assigning generation and load values to nodes.
- Path Determination: Using optimization or heuristic methods to determine the most efficient routes for power flow.
- Flow Adjustment: Iteratively adjusting flows to ensure no component exceeds its capacity while meeting demand.

Capacity constrains are also considering when distributing the flows in the Electricity Power System (EPS). When network components approach capacity limits, various strategies are employed (Powell, 2004):
- Redispatch: Adjusting generation to alleviate congestion.
- Load Shedding: Reducing demand in critical areas.
- Flow Control Devices: Using Flexible AC Transmission System (FACTS) devices to redistribute power flows.

Energy losses, a critical aspect of electricity networks, are calculated based on the current in each line, typically modeled as proportional to the square of the current. These models help quantify losses and identify inefficiencies within the network.

Finally, the results are often visualized using load flow diagrams and heatmaps that depict voltage profiles, power flows, and congestion points. These visual tools assist in identifying bottlenecks and planning network upgrades. By employing these methodologies, electricity flow allocation models enable efficient and reliable

This project has received funding from the European Union's Horizon Europe research and innovation programme under grant agreement No. 101093854

operation of power systems, supporting both short-term operations and long-term planning.

## Natural gas network

The natural gas system (NGS) requires accurate flow allocation models to simulate the movement of gas from production sites to consumers. These models account for various network components, including transmission pipelines, compressor stations, and storage facilities. The modeling approach for flow allocation is influenced by factors such as the available data, the network topology, and the required level of detail. Typically, NGSs consist of natural gas wells, high-pressure and low-pressure transmission pipelines, compressors, storage facilities, and gas consumers (including residential, commercial, and industrial sectors). A critical component of the industrial sector is gas-fired power plants, which serve as significant gas loads and link the electric power systems (EPSs) with NGSs. The network elements are connected through nodes representing key points in the system, where gas pressures are associated. Natural gas suppliers and consumers are modeled as positive and negative gas injections at the respective nodes. Pipelines are represented as edges that carry the natural gas flow.

The gas flow allocation model is based on the following equations (Pantoš, 2011).

- Gas Supply: Each natural gas supplier is modeled as a positive gas injection limited by maximum and minimum capacity. The equation for node *i* is:

$$v_i^{min} \leq v_i \leq v_i^{max} \quad [27]$$

- Gas loads are represented as negative gas injections limited by upper and lower limits, in case of node i:

$$L_i^{min} \leq L_i \leq L_i^{max} \quad [28]$$

- Gas storages are categorized based on their capacity and operating parameters. However, for the Market-based congestion management (MBCM) of EPSs, they are either modeled as loads or suppliers, thus their capacities are limited as in Eq 36 and 37. The exceptions are self-owned storage facilities of gas-fired power plants, as discussed later in the paper.

The flow of natural gas through pipelines depends on several factors, including nodal pressures, pipeline characteristics (such as length, diameter, temperature, pressure, and roughness), and gas properties. The mathematical model for gas flow from node *i* to node *j* is given by:

$$f_{ij} = sgn(\pi_i, \pi_j) \cdot C_{ij} \cdot \sqrt{\pi_i^2 - \pi_j^2} \quad [29]$$

This project has received funding from the European Union's Horizon Europe research and innovation programme under grant agreement No. 101093854

$$sgn(\pi_i, \pi_j) = \begin{cases} 1 & \pi_i \geq \pi_j \\ -1 & \pi_i < \pi_j \end{cases} \quad [30]$$

where $C_{ij}$ is the pipeline *i-j* constant that depends on temperature, length, diameter, friction and gas composition.

To mitigate pressure losses caused by pipeline resistance, compressor stations are installed at various points along pipelines. The flow of gas through a centrifugal compressor between nodes *i* and *j* is modeled as:

$$f_{ij} = sgn(\pi_i, \pi_j) \cdot \frac{H_{ij}}{a_{ij} - b_{ij} \cdot \left[\frac{\max(\pi_i, \pi_j)}{\min(\pi_i, \pi_j)}\right]^{\alpha_{ij}}} \quad [31]$$

where $a_{ij}$, $b_{ij}$ and $\alpha_{ij}$ are empirically obtained parameters corresponding to the compressor *i-j* design. $H_{ij}$ represents the power of compressor *i-j* as a control variable, where maximum and minimum values have to be considered:

$$H_{ij}^{min} \leq H_{ij} \leq H_{ij}^{max} \quad [32]$$

Additionally, the pressure ratio in Eq 40 is restricted within a feasible range in Eq. 41, which is based on compressor characteristics:

$$R_{ij}^{min} \leq \frac{\max(\pi_i, \pi_j)}{\min(\pi_i, \pi_j)} \leq R_{ij}^{max} \quad [33]$$

Compressor stations consume additional gas to operate, which is withdrawn from either the inlet node i or outlet node j of the compressor. The natural gas consumed by the compressor to power the turbines is represented as $F_{ij}$, and it is related to the compressor power $H_{ij}$ by:

$$F_{ij} = k_{ij} + d_{ij} \cdot H_{ij} + e_{ij} \cdot H_{ij}^2 \quad [34]$$

where $k_{ij}$, $d_{ij}$ and $e_{ij}$ are the natural gas consuming parameters of compressor *i-j.*

At each node, the gas flow must balance, meaning that the total gas injected into the node must equal the total gas withdrawn. The steady-state gas flow mismatch is modeled as zero:

$$g(v, \pi, H, L) = A \cdot v - B \cdot L - D \cdot f - G \cdot F = 0 \quad [35]$$

or for node i:

$$g_i(v, \pi, H, L) = \sum_{j=1}^{NGS} A_{ij} \cdot v_j - \sum_{j=1}^{NGS} B_{ij} \cdot L_j - \sum_{j \in GC_i} f_{ij} - \sum_{j=1}^{NC} G_{ij} \cdot F_{ij} = 0 \quad [36]$$

In this system, NGS represents the number of gas suppliers, NN is the number of nodes in the system, NC is the number of compressors, and NGL is the number of gas loads. These equations represent a set of nonlinear equations, where variables such as node pressure, compressor power, gas supply, and gas load are interdependent. This mathematical framework facilitates the optimization and simulation of gas flow across the entire network, helping to ensure efficient distribution and minimize

This project has received funding from the European Union's Horizon Europe research and innovation programme under grant agreement No. 101093854

congestion.

### Telecommunications network

Generally, in telecoms networks there are no capacity issues as long as connectivity is maintained (Oughton et al., 2016). Hence, the flow model for telecoms involves understanding how much demand in terms of customers (infrastructures, households and businesses) can be associated with telecoms assets. Demands are allocated to exchanges, macro cells, and telecom masts based on the dependency links established between them and nearby dependent assets from other sectors, using notional proximity connections within their respective service areas. For exchanges and macro cells, each node is assumed to serve the closest ports, intermodal stations, airports, and power nodes, resulting in the creation of Voronoi polygons that define their service boundaries. Similarly, railways are segmented and assigned to the nearest telecom masts to ensure effective connectivity.

This systematic allocation approach reflects realistic coverage scenarios, providing a structured representation of how demands are distributed across interconnected assets in the network. The detailed interdependency connection procedure is further elaborated in Section 3e, offering a comprehensive view of how these links are established and maintained.

### Flow exchanges between electricity and gas

The electricity produced by gas-fired power plants is a nonlinear function of the gas supply. The amount of natural gas (denoted as $L_j$) needed to produce a certain amount of power (denoted as $P_j$) is given by the formula (Pantoš, 2011):

$$L_j = p_j + q_j \cdot P_j + r_j \cdot P_j^2 \qquad [37]$$

where coefficients $p_j, q_j$ and $r_j$ depend on the power plant characteristics.

Each gas-fired power plant has a minimum and maximum production capacity, which also depends on the natural gas supply contracts it has with suppliers. Although these contracts may impose additional constraints, this study will assume that the plant’s operational limits already account for any restrictions from those contracts.

Gas storage facilities are treated as either gas loads or suppliers, with limitations on their capacities. Self-owned storage at gas-fired plants doesn’t directly affect the gas network because it acts as an energy buffer. Thus, the plant’s characteristics are adjusted in the gas consumption models, but the storage itself isn’t modeled separately.

This project has received funding from the European Union’s Horizon Europe research and innovation programme under grant agreement No. 101093854

Gas-fired power plants also participate in Market-based Congestion Management (MBCM), where they submit bids to the system operator. Each bid includes the amount of power offered, the price, and the time. Since natural gas prices affect the generation costs, these prices are considered in the bidding process. However, the model assumes that any cost impacts of redispatching, including natural gas supply costs, are already reflected in the bids submitted for MBCM. Therefore, the model only uses the prices provided in the MBCM bids.

# 5. Conclusions and future opportunities

## 5.1. Limitations

This study offers a detailed, pan-European analysis of interdependent infrastructure networks, marking a significant step forward in the field. To the best of our knowledge, the breadth of data collection and the modeling of multiple interconnected infrastructure systems at this scale is unprecedented. The failure analysis adds a unique dimension by systematically identifying cascading failures and illustrating how disruptions propagate across networks. However, we recognize several limitations in the current approach, stemming from the study's scope and proof-of-concept nature:

- Data Availability and Coverage: Accurate data on asset locations and network topologies is not always accessible. For example, smaller operators in the telecoms and electricity sectors are underrepresented in the model.
- Interdependency Data: There is a scarcity of reliable data on cross-network interdependencies, leading to assumptions that may simplify complex relationships.
- Redundancy Estimations: Limited data within and between networks complicates the estimation of built-in redundancies, potentially underestimating system resilience.
- Flow Assignments: Flow assignments rely on a simplistic approach, using Eurostat and ENTSO databases. While this ensures replicability, dynamic models could better capture real-time network behaviors.
- Failure Scenarios: The analysis tests single points of failure only. Real-world scenarios often involve multiple simultaneous failures, which would offer a more comprehensive understanding of cascading impacts.

This foundational work demonstrates the potential of integrated, large-scale modeling while highlighting areas for future research and data enhancement.

## 5.2. What this report covers and what it does not

The report does provide:

This project has received funding from the European Union's Horizon Europe research and innovation programme under grant agreement No. 101093854

- A methodology to map and define cross-sectorial and intermodal transportation dependencies, offering insights into how sectors and transport modes interact.
- A framework for exploring failure propagation within an already mapped cross-sectorial network, highlighting cascading impacts.
- A set of impact resilience metrics that assess asset-level disruptions and the cascading impacts across networks and sectors, accounting for functionality loss and supporting the development of targeted resilience strategies.

The report does not provide:

- Data to replicate any infrastructure network at the local or sectoral level. Theoretically the model could be applied at local scales. However, for this project it is intended to operate at a pan-European scale and might not capture local nuances or specific regional systems.
- A substitute for comprehensive sector-specific modeling, as it relies on general assumptions and publicly available data.
- A complete representation of all network interdependencies, particularly for smaller operators or private entities with limited publicly available information.
- A dynamic real-time simulation, as the flow assignments and interdependencies are primarily static and derived from high-level datasets.

## 5.3. Next steps of development

This study introduces a model for assessing infrastructure resilience by integrating interdependent energy, transport, and digital networks across Europe. To enhance its capabilities and utility, the following development directions align with specific work packages (WPs), ensuring a structured pathway for progress:

- Enhanced Data Collection: Expanding datasets across sectors will improve the model's analytical precision. These efforts directly address WP1 objectives to standardize and enrich the data input pipeline.
    - Digital networks: Focus on smaller providers and connectivity data to address gaps in communication networks.
    - Energy systems: Include detailed data on electricity and gas distribution networks.
    - Interdependencies: Collect cross-network redundancy information.
- Investigating software and hardware interdependencies within critical systems will improve the model's ability to assess cyber vulnerabilities. WP2 can focus on developing frameworks to capture these dependencies.
- Compound Risks: Expanding risk analysis to spatially compound hazards and consecutive events will enhance WP2's focus on multi-risk scenarios.
- Global Interdependencies: Future work could analyze global connectivity impacts, aligning with WP3's mandate to study international and economic interdependencies.

This project has received funding from the European Union's Horizon Europe research and innovation programme under grant agreement No. 101093854

- Supply Chain Impacts: Incorporating supply chain disruptions will provide a comprehensive analysis of economic consequences, furthering WP3 objectives.
- Dynamic Network Models: Developing process-based models to track failure evolution across systems supports WP4 goals. Metrics such as service disruption, customer impacts, and economic losses will be incorporated into simulations.
- Coping, Repair, and Recovery Strategies: WP4 can extend its focus to adaptive repair mechanisms and faster recovery strategies, broadening resilience modeling.
- Improved Information Sharing: Initiatives for cross-sector data sharing align with WP5's focus on collaborative frameworks and stakeholder engagement.
- Integration with Long-term Planning: Expanding scenarios across sectors and embedding resilience into future policy objectives supports WP5's aim to integrate research insights into practical EU infrastructure planning.
- Critical Asset Mapping: Applying the methodology to prioritize lifelines and critical assets will assist WP5 in guiding resilience investments effectively.
- Validation Through Empirical Data: Incorporating real-world failure scenarios aligns with WP6's efforts to enhance model credibility and stakeholder trust.
- Documentation for Broader Use: Making tools and datasets accessible through Jupyter Notebooks or similar platforms will further WP6's mission of promoting usability and knowledge sharing.

By aligning these next steps with the work packages, this study can systematically enhance its scope and impact, fostering a robust framework for infrastructure resilience across Europe.

# References

2004/54/EC. (n.d.). Directive 2004/54/EC of the European Parliament and of the Council of 29 April 2004 on minimum safety requirements for tunnels in the Trans-European Road Network.

Buldyrev, S. V., Parshani, R., Paul, G., Stanley, H. E., & Havlin, S. (2010). Catastrophic cascade of failures in interdependent networks. Nature, 464(7291), 1025–1028. https://doi.org/10.1038/nature08932

Cohen, E. A., & Barabási, A.-L. (2002). Linked: The New Science of Networks. Foreign Affairs, 81(5), 204. https://doi.org/10.2307/20033300

Diettrich, J. C., Pluta, W., & Medrjoubi, W. (n.d.). The merged IGGIELGN dataset [Dataset].

European Environment Agency (Ed.). (2000). Are we moving in the right direction? Indicators on transport and environment integration in the EU. Office for Official Publ. of the Europ. Communities.

Eurostat. (n.d.). Eurostat Transport Datasets [Dataset]. https://ec.europa.eu/eurostat/web/transport/database

G. W. Stagg, & A. H. El-Abiad. (1968). Computer Methods in Power System Analysis. McGraw-Hill Education.

Grainger, J., & Stevenson, W. D. (1994). Power System Analysis. McGraw-Hill Education.

Hall, J. W., Tran, M., Hickford, A. J., & Nicholls, R. J. (2016). The Future of National Infrastructure: A System-of-Systems Approach. Cambridge University Press.

Kesete, Y. Y., Raffo, V., Pant, R., Koks, E. E., Paltan, H., Russell, T., & Hall, J. W. (2021). Climate Change Risk Analysis of Argentina's Land Transport Network. World Bank. https://doi.org/10.1596/36504

Kivela, M., Arenas, A., Barthelemy, M., Gleeson, J. P., Moreno, Y., & Porter, M. A. (2014). Multilayer networks. Journal of Complex Networks, 2(3), 203–271. https://doi.org/10.1093/comnet/cnu016

Koks, E., Rozenberg, J., Tariverdi, M., Dickens, B., Fox, C., Van Ginkel, K., & Hallegatte, S. (2023). A global assessment of national road network vulnerability. Environmental Research: Infrastructure and Sustainability, 3(2), 025008. https://doi.org/10.1088/2634-4505/acd1aa

Kundur, P. (1994). Power System Stability and Control. McGraw-Hill Education.

L, P. (2004). Power System Load Flow Analysis. McGraw-Hill Education.

Leontief, W. W. (1951). Input-Output Economics. SCIENTIFIC AMERICAN, 185(4), 15–21.

Lewis, Ted G. (2011). Network science: Theory and applications.

Mühlhofer, E., Bresch, D. N., & Koks, E. E. (2024). Infrastructure failure cascades quintuple risk of storm and flood-induced service disruptions across the globe. One Earth, 7(4), 714–729. https://doi.org/10.1016/j.oneear.2024.03.010

Oh, J. E., Espinet Alegre, X., Pant, R., Koks, E. E., Russell, T., Schoenmakers, R., & Hall, J. W. (2019). Addressing climate change in transport: Volume 2: Pathway to Resilient Transport. World Bank. http://hdl.handle.net/10986/32412

OpenStreetMap contributors. (2017). [Dataset]. https://planet.osm.org

Oughton, E. J., Tran, M., Jones, C. B., & Ebrahimy, R. (2016). Digital communications and information systems. In J. W. Hall, M. Tran, A. J. Hickford, & R. J. Nicholls

This project has received funding from the European Union's Horizon Europe research and innovation programme under grant agreement No. 101093854

(Eds.), The Future of National Infrastructure (1st ed., pp. 181–202). Cambridge University Press. https://doi.org/10.1017/CBO9781107588745.010

Pant, R., Hall, J. W., & Blainey, S. P. (2016). Vulnerability assessment framework for interdependent critical infrastructures: Case-study for Great Britain's rail network. European Journal of Transport and Infrastructure Research. https://doi.org/10.18757/EJTIR.2016.16.1.3120

Pant, R., Li, Y., & Hall, j. W. (2024). Reviewing and informing the existing gaps for Critical Infrastructure interdependencies. MIRACA Task 2.1 report.

Pant, R., Russell, T., Zorn, C., & Hall, J. W. (2020). Resilience Study Research for NIC (No. April). April, Article April.

Pantoš, M. (2011). Market-based congestion management in electric power systems with increased share of natural gas dependent power plants. Energy, 36(7), 4244–4255. https://doi.org/10.1016/j.energy.2011.04.019

Poljanšek, K., Bono, F., & Gutiérrez, E. (2012). Seismic risk assessment of interdependent critical infrastructure systems: The case of European gas and electricity networks. Earthquake Engineering & Structural Dynamics, 41(1), 61–79. https://doi.org/10.1002/eqe.1118

Rose, A. (2004). Defining and measuring economic resilience to disasters. Disaster Prevention and Management: An International Journal, 13(4), 307–314. https://doi.org/10.1108/09653560410556528

Speth, D., Sauter, V., Plötz, P., & Signer, T. (2022). Synthetic European road freight transport flow data. Data in Brief, 40, 107786. https://doi.org/10.1016/j.dib.2021.107786

Thacker, S., Pant, R., & Hall, J. W. (2017a). System-of-systems formulation and disruption analysis for multi-scale critical national infrastructures. Reliability Engineering and System Safety, 167(April), Article April. https://doi.org/10.1016/j.ress.2017.04.023

Thacker, S., Pant, R., & Hall, J. W. (2017b). System-of-systems formulation and disruption analysis for multi-scale critical national infrastructures. Reliability Engineering and System Safety, 167(April), Article April. https://doi.org/10.1016/j.ress.2017.04.023

Thacker, S., Pant, R., & Hall, J. W. (2018). Preserving key topological and structural features in the synthesis of multi-level electricity networks for modeling of resilience and risk. Ournal of Infrastructure Systems, ASCE, 24. https://doi.org/10.1061/(ASCE)IS.1943-555X.0000404

The UNECE E-Rail Census: Interactive Map of Annual Average Daily Traffic Collected on the E-Rail Network. (2017). [Dataset]. https://unece.org/traffic-census-map-0

Thompson, D. A., Glenn, D. E., Trethewey, L. L., Blackett, P., & Logan, T. M. (2024). Capturing cascading consequences is required to reflect risk from climate change and natural hazards. Climate Risk Management, 44, 100613. https://doi.org/10.1016/j.crm.2024.100613

TRUST_model_2024. (n.d.).

UNECE. (2017). The UNECE E-Road Census: Interactive Map of Annual Average Daily Traffic Collected on the E-Road Network [Dataset]. https://unece.maps.arcgis.com/apps/webappviewer/index.html?id=cf22916b3df741368b8f234d4390e90b

This project has received funding from the European Union's Horizon Europe research and innovation programme under grant agreement No. 101093854

UNECE. (2022). The UNECE E-IWW Census: Interactive Map of Inland Waterways Network [Dataset]. https://gis.unece.org/portal/apps/webappviewer/index.html?id=56e9186ac6e8400f8e3177957a72b9ab
Verschuur, J., Koks, E. E., & Hall, J. W. (2022). Ports' criticality in international trade and global supply-chains. Nature Communications, 13(1), Article 1. https://doi.org/10.1038/s41467-022-32070-0
Verschuur, J., Pant, R., Koks, E., & Hall, J. (2022). A systemic risk framework to improve the resilience of port and supply-chain networks to natural hazards. Maritime Economics and Logistics, 24(3), Article 3. https://doi.org/10.1057/s41278-021-00204-8
Wood, A. J., Wollenberg, B. F., Shebl&  eacute, & Gerald B. (n.d.). Power Generation, Operation and Control.
Xie, W., Rose, A., Li, S., He, J., Li, N., & Ali, T. (2018). Dynamic Economic Resilience and Economic Recovery from Disasters: A Quantitative Assessment. Risk Analysis, 38(6), 1306–1318. https://doi.org/10.1111/risa.12948
Zorn, C., Pant, R., Thacker, S., & Shamseldin, A. Y. (2020). Evaluating the magnitude and spatial extent of disruptions across interdependent national infrastructure networks. ASCE-ASME Journal of Risk and Uncertainty in Engineering Systems, Part B: Mechanical Engineering, 6(2), Article 2. https://doi.org/10.1115/1.4046327

This project has received funding from the European Union's Horizon Europe research and innovation programme under grant agreement No. 101093854